

# Cosmological dynamics of mimetic gravity

Jibitesh Dutta<sup>a,b</sup> Wompherdeiki Khylllep<sup>c,d</sup> Emmanuel N. Saridakis<sup>e,f,g</sup> Nicola Tamanini<sup>h,i</sup> and Sunny Vagnozzi<sup>j,k</sup>

<sup>a</sup>Mathematics Division, Department of Basic Sciences and Social Sciences, North Eastern Hill University, NEHU Campus, Shillong, Meghalaya 793022, India

<sup>b</sup>Inter University Centre for Astronomy and Astrophysics(IUCAA), Pune 411 007, India

<sup>c</sup>Department of Mathematics, North Eastern Hill University, NEHU Campus, Shillong, Meghalaya 793022, India

<sup>d</sup>Department of Mathematics, St. Anthony's College, Shillong, Meghalaya 793001, India

<sup>e</sup>Chongqing University of Posts & Telecommunications, Chongqing, 400065, China

<sup>f</sup>Department of Physics, National Technical University of Athens, Zografou Campus GR 157 73, Athens, Greece

<sup>g</sup>CASPER, Physics Department, Baylor University, Waco, TX 76798-7310, USA

<sup>h</sup>Max-Planck-Institut für Gravitationsphysik, Albert-Einstein-Institut, Am Mühlenberg 1, 14476 Potsdam-Golm, Germany

<sup>i</sup>Laboratoire Astroparticule et Cosmologie, CNRS UMR 7164, Université Paris-Diderot, 10 rue Alice Domon et Léonie Duquet, 75013 Paris, France

<sup>j</sup>The Oskar Klein Centre for Cosmoparticle Physics, Department of Physics, Stockholm University, SE-106 91 Stockholm, Sweden

<sup>k</sup>The Nordic Institute for Theoretical Physics (NORDITA), Roslagstullsbacken 23, SE- 106 91 Stockholm, Sweden

E-mail: [jibitesh@nehu.ac.in](mailto:jibitesh@nehu.ac.in), [sjwomkhylllep@gmail.com](mailto:sjwomkhylllep@gmail.com),  
[Emmanuel\\_Saridakis@baylor.edu](mailto:Emmanuel_Saridakis@baylor.edu), [nicola.tamanini@aei.mpg.de](mailto:nicola.tamanini@aei.mpg.de),  
[sunny.vagnozzi@fysik.su.se](mailto:sunny.vagnozzi@fysik.su.se)

**Abstract.** We present a detailed investigation of the dynamical behavior of mimetic gravity with a general potential for the mimetic scalar field. Performing a phase-space and stability analysis, we show that the scenario at hand can successfully describe the thermal history of the universe, namely the successive sequence of radiation, matter, and dark-energy eras. Additionally, at late times the universe can either approach a de Sitter solution, or a scaling accelerated attractor where the dark-matter and dark-energy density parameters are of the same order, thus offering an alleviation of the cosmic coincidence problem. Applying our general analysis to various specific potential choices, including the power-law and the exponential ones, we show that mimetic gravity can be brought into good agreement with the observed behavior of the universe. Moreover, with an inverse square potential we find that mimetic gravity offers an appealing unified cosmological scenario where both dark energy and dark matter are characterized by a single scalar field, and where the cosmic coincidence problem is alleviated.

**Keywords:** Mimetic gravity, dark energy, dark matter, dynamical analysis, coincidence problem

---

## Contents

<b>1</b>	<b>Introduction</b>	<b>1</b>
<b>2</b>	<b>Mimetic gravity and cosmology</b>	<b>3</b>
<b>3</b>	<b>Dynamical system analysis</b>	<b>7</b>
3.1	Mimetic gravity with a general scalar field potential	8
3.2	Mimetic gravity with an inverse square potential	11
3.3	Mimetic gravity with a power-law or exponential potential	15
3.4	Mimetic gravity with $V(\phi) \propto (1 + \beta\phi^2)^{-2}$	17
<b>4</b>	<b>Cosmological implications</b>	<b>19</b>
<b>5</b>	<b>Conclusions</b>	<b>20</b>
<b>A</b>	<b>Appendix: stability analysis for <math>A_1, A_2</math></b>	<b>21</b>
A.1	Case: $w \neq 0$	21
A.2	Case: $w = 0$	22
<b>B</b>	<b>Appendix: stability analysis for <math>A_{3\pm}</math></b>	<b>22</b>

---

## 1 Introduction

The dark universe picture, astonishingly confirmed by a variety of experiments and surveys in the past years [1–3], paints a rather peculiar picture of the universe we live in. In particular, observations indicate that around 25% of the energy budget of the universe corresponds to the dark matter sector, while around 70% constitutes the dark energy one [4], with both sectors being relatively unknown for the moment. Concerning dark matter, there have been numerous attempts to attribute it to specific candidates [5], such as a weakly interacting massive particle [6], while several theories instead posit the existence of additional particles and forces beyond those of the Standard Model (e.g. [7–12]).

On the other hand, the description of dark energy is more uncertain, since if it does not correspond to the simplest choice of a cosmological constant (which nonetheless is problematic from a theoretical point of view [13, 14]), then there are essentially two ways to explain it. Firstly, assuming that general relativity correctly describes gravity on both galactic and cosmological scales, one can attribute dark energy to various fields or exotic matter and energy components (for reviews see [15, 16]). However, a second intriguing possibility is that general relativity might not in fact be the correct theory of gravity on all scales, thus paving the road for the wide plethora of modified gravity theories (for reviews see [17–22]). Modified theories of gravity are theoretically and observationally appealing, and ever-increasingly sensitive and precise upcoming surveys provide the exciting possibility of robustly testing these theories against observational data.

One interesting class of modified gravity is the mimetic gravitational construction, which has been proposed in 2013 [23] and has received considerable attention since then. In its original formulation the mimetic theory of gravity can be obtained starting from general

relativity, by isolating the conformal degree of freedom of gravity in a covariant fashion through a re-parametrization of the physical metric in terms of an auxiliary metric and a mimetic field. It is then shown that the resulting gravitational field equations feature an additional term sourced by the mimetic field, which can be interpreted as the contribution of a pressureless perfect fluid. It is furthermore shown that, on a Friedmann-Robertson-Walker (FRW) background, this fluid behaves precisely as a dust component. Thus, the mimetic field can mimic cold dark matter on cosmological scales, a feature that gave the theory its name.

Several extensions of the basic mimetic gravity have been proposed and studied in detail in the literature (for a review see [24]). The earliest extension proposed, motivated by possible caustic instabilities, was based on a Proca-like vector field [25]. Motivated instead by possible ghost instabilities, a mimetic tensor-vector-scalar theory was presented in [26]. Another interesting generalization envisions the addition of a potential  $V(\phi)$  for the mimetic scalar field [27]. It was shown that in such a way it is possible to mimic any given cosmological background evolution by a suitable choice of the potential. Other extensions have been carried out adding higher-order curvature invariants, motivated by the fact that such terms usually appear in the low-energy effective gravitational action when quantum or stringy corrections are taken into account. The example *par excellence* in this sense is mimetic  $F(R)$  gravity [28, 29], where the same procedure leading to mimetic gravity from general relativity is applied to the  $F(R)$  gravitational framework. In the same spirit, other modifications to the curvature sector of mimetic action have led to different proposed extensions (see e.g. [30] for one of the first extensions), such as mimetic  $f(R, T)$  [31], mimetic  $f(G)$  [32], mimetic  $f(R, \phi)$  [33], mimetic covariant Hořava-like gravity [34, 35], mimetic Horndeski gravity [35, 36], mimetic Galileon gravity [37, 38], non-local mimetic  $F(R)$  gravity [39], unimodular-mimetic  $F(R)$  gravity [40], and mimetic Born-Infeld gravity [41, 42]. The impact of higher-derivative terms in the mimetic gravity action was then studied in [43, 44], as well as in [45–47], and motivated by instability issues in the recent works [48–52]. Other extensions of mimetic gravity include bi-scalar mimetic models [53], vector-tensor mimetic gravity [54], braneworld mimetic gravity [55], and extensions implementing the limiting curvature hypothesis and hence constructed to resolve cosmological singularity issues [56, 57]. Finally, models in which the mimetic field is non-minimally coupled to matter [58] and baryon number [59] currents (in the latter case in order to enable baryogenesis) have been also studied.

Apart from the basic construction of a mimetic model one may analyze the perturbations and the stability of the theory [27, 31, 35, 43–52, 60–65]. Several recent works have pointed out that mimetic gravity might suffer from ghost instabilities (although not of the type associated to higher derivative instability, such as the Ostrogradsky ghost), as well as gradient instabilities, in the scalar and/or tensor sectors [25, 26, 48–52, 61–71]. Although currently a lack of consensus regarding these issues persists, it is worth pointing out that if mimetic gravity does indeed suffer from instabilities then there are ways to rescue the theory, e.g. by directly coupling higher derivatives of the mimetic field to curvature.

Mimetic gravity can have interesting cosmological applications. Numerous works have investigated in detail the cosmological phenomenology of the above constructions, such as inflation, late-time acceleration, and unified universe evolution including the intermediate radiation and matter eras [27–29, 31–41, 47–60, 72–76]. In particular [77] focused on cosmological attractors. Additionally, in the above framework one can study black hole solutions [78–80], compact “stellar” objects which solve the Tolman-Oppenheimer-Volkoff equations [81], quark and neutron stars [82], wormholes [83], modifications to the local gravitational potential which can potentially explain the flatness of rotation curves [58, 83], and gravitational

focusing of mimetic matter [84]. Finally, confronting the theory with observations, one can use data from large-scale structure [85] and gravitational waves [86, 88–93] surveys.

It has also been realized that mimetic gravity is intimately connected to a number of other well-known theories of modified gravity. Perhaps the most remarkable connection is the one which considers mimetic gravity to appear in the infrared limit of the projectable version of Hořava-Lifshitz gravity. This correspondence has been formally proven in [61] and shows that mimetic gravity can be viewed as the low-energy limit of a (Lorentz-violating) theory of quantum gravity. Intimate relations between mimetic gravity and other theories include connections to the scalar Einstein-Aether theory [37, 94], Hořava-like theories with dynamical diffeomorphism invariance breaking [34], degenerate higher-order scalar-tensor theories beyond Horndeski [66], singular Brans-Dicke theory [74], non-commutative geometry [95], effective implementations of the limiting curvature criterion [52, 56, 57, 62, 96], as well as to other more exotic theories of gravity [47, 97–101].

In the present work we are interested in performing a complete dynamical analysis of the cosmological evolution in mimetic gravity, since although mimetic cosmology has been extensively studied, the dynamical behavior of these solutions has not been explored in detail (apart from the sub-class of mimetic  $F(R)$  gravity [29]). Dynamical systems analysis provides a very powerful tool in the study of the asymptotic behavior as well as of the complete cosmological dynamics of a given cosmological model [102–105]. This phase-space and stability examination allows to bypass the non-linearities of the cosmological equations, and obtain a description of the global dynamics independently of the initial conditions of the universe, connecting critical points to epochs of the evolutionary history which are of particular relevance. In particular, a late-time period of accelerated expansion would typically correspond to a late-time attractor, whereas epochs of radiation and matter domination typically correspond to saddle points. With the full machinery of dynamical systems is indeed possible to investigate the complete dynamics of any cosmological model, provided suitable dynamical variables can be identified. Hence, these powerful methods have been extensively applied to analyse the evolution of several cosmological models, including many modified gravity scenarios (see e.g. [106–124] for some recent works).

This paper is organized as follows: In section 2 we provide a review of mimetic gravity, and we apply it within a cosmological framework. In section 3 we perform a detailed phase-space and stability analysis of mimetic cosmology for a general potential, and then we specify the investigation in the case of various specific potentials, amongst others for the power-law and the exponential ones. In section 4 we discuss the cosmological implications of the obtained results. Finally, section 5 is devoted to the conclusions.

## 2 Mimetic gravity and cosmology

In this section we briefly review the current status of mimetic gravity. For further details, we refer the reader to the recent review [24]. In its original formulation the mimetic theory of gravity can be obtained starting from general relativity. In particular, isolating the conformal degree of freedom of gravity in a covariant fashion by parametrizing the physical metric  $g_{\mu\nu}$  in terms of an auxiliary metric  $\tilde{g}_{\mu\nu}$  and the mimetic field  $\phi$ , one can write [23]

$$g_{\mu\nu} = \tilde{g}_{\mu\nu} \tilde{g}^{\alpha\beta} \partial_\alpha \phi \partial_\beta \phi. \quad (2.1)$$

This mimetic parametrization makes it clear that the physical metric is invariant under conformal transformations of the auxiliary metric. It is easy to show that, for consistency, the

following condition on the gradient of the mimetic field has to be satisfied [23]

$$g^{\mu\nu}\partial_\mu\phi\partial_\nu\phi = 1. \quad (2.2)$$

The consistency condition (2.2) can be implemented at the level of the action through a Lagrange multiplier constraint as [27]

$$I = \int d^4x\sqrt{-g} \left[ \frac{R}{2\kappa^2} + \lambda(\partial^\mu\phi\partial_\mu\phi - 1) + \mathcal{L}_m \right], \quad (2.3)$$

where  $\kappa^2$  is the gravitational constant,  $R$  is the Ricci scalar, and  $\mathcal{L}_m$  is the usual standard-model matter Lagrangian, and thus variation of the action with respect to the Lagrange multiplier field  $\lambda$  enforces the validity of the constraint (2.2) (actions featuring Lagrange-multiplier constrained scalar fields are in general being used in the literature, see for instance [125–127]).

As we mentioned in the Introduction, a simple extension of the original mimetic construction (2.3) is to include a potential for the mimetic field. In particular, one writes [27]

$$I = \int d^4x\sqrt{-g} \left[ \frac{R}{2\kappa^2} - \frac{\lambda}{2}(\partial^\mu\phi\partial_\mu\phi - 1) + V(\phi) + \mathcal{L}_m \right], \quad (2.4)$$

where  $V(\phi)$  is the self-interacting scalar field potential, and where the factor of 1/2 in front of the Lagrange multiplier  $\lambda$  is introduced for convenience. Such a model has been shown to provide an economical way of reproducing a number of simple and well-motivated cosmological scenarios, relevant for both early- and late-time cosmology, without the need for neither an explicit dark matter nor a dark energy fluid [27]. Moreover, one can obtain late-time accelerating solutions, early-time inflationary states, bouncing solutions, etc. It is interesting to mention that the above model is consistent with the latest observation of the gravitational wave event GW170817 from a binary neutron star inspiral with an electromagnetic counterpart event [143], as the corresponding propagation speed of tensor perturbations is identically equal to the speed of light [86, 92, 93].

The equations of motion of the theory can be obtained by varying the action with respect to the physical metric, however taking into account its dependence on the auxiliary metric and the mimetic field. Hence, variation of the action (2.4) with respect to the metric gives

$$\frac{1}{\kappa^2}G_{\mu\nu} = \lambda\partial_\mu\phi\partial_\nu\phi + g_{\mu\nu}V(\phi) + T_{\mu\nu}, \quad (2.5)$$

where  $G_{\mu\nu}$  is the Einstein tensor and  $T_{\mu\nu}$  is the standard-model matter energy-momentum tensor. On the other hand, as we mentioned, variation with respect to the Lagrange multiplier indeed yields condition (2.2). Taking the trace of equation (2.5) we find the Lagrange multiplier to be

$$\lambda = \left( \frac{G}{\kappa^2} - T - 4V \right), \quad (2.6)$$

where  $G$  and  $T$  are the traces of the Einstein tensor and the matter energy-momentum tensor respectively. Finally, variation of the action (2.4) with respect to the mimetic field  $\phi$  gives

$$\nabla^\mu(\lambda\partial_\mu\phi) + \frac{dV}{d\phi} = 0, \quad (2.7)$$

an equation that can alternatively be derived taking the covariant derivative of Eq. (2.5) and employing the Bianchi identity  $\nabla^\mu G_{\mu\nu} = 0$  together with the conservation equation  $\nabla^\mu T_{\mu\nu} = 0$ .

It is worth mentioning that one can substitute the value of  $\lambda$  obtained from Eq. (2.6) into the other field equations. This operation would eliminate  $\lambda$  from the dynamics and the resulting system of equations would involve in its place some combination of the degrees of freedom of the metric, the matter fluid and the mimetic field. In practice one does not gain any advantage by this operation since no additional dynamics is obtained, and computationally one ends up dealing with more complex expressions. Moreover, this operation would lead to the field equations of the original formulation of mimetic gravity theory without the Lagrange’s multiplier  $\lambda$  and this would invalidate the very purpose of taking action (2.3) (for details see [24]). For these reasons in what follows we prefer to explicitly work with  $\lambda$  rather than eliminating it for more complicated expressions.

From equations (2.5)-(2.7) it is clear that the gravitational field equations in mimetic gravity differ from those of general relativity by the presence of an extra source term which mimics a perfect fluid. In the original version of the theory, where the potential is absent, this extra fluid has energy density  $\rho_f = \frac{G}{\kappa^2} - T$ , four-velocity  $\partial_\mu\phi$  and pressure  $p_f = 0$ . The fact that  $p_f = 0$  suggests that this extra term can play the role of a pressureless fluid and hence mimic a dust-matter component on cosmological scales. Therefore, the construction at hand can mimic cold dark matter on cosmological scales, bypassing the need for an additional dark matter component, that is why it is called “mimetic gravity”.

The foremost questions to be addressed is why did the seemingly innocuous reparametrization of the physical metric in Eq. (2.1) lead to different equations of motion compared to general relativity. Early attempts to address this question identified the dark matter degree of freedom as arising from gauging the local Weyl invariance of the theory [25], whereas other early works explained the different equations of motion in terms of variation of the action over a restricted class of functions which results in a broader freedom in the dynamics of the theory [128]. Nowadays it is well understood that the reason behind the fact that the equations of motion of mimetic gravity differ from those of general relativity, is to be sought in the fact that the former is related to the latter via a singular (i.e. non-invertible) disformal transformation. Recalling that general relativity satisfies diffeomorphism invariance allows one to reparametrize the physical metric in terms of an auxiliary metric and a scalar field through what is known as a disformal transformation [129]. An invertible disformal transformation returns a theory which is equivalent to general relativity. On the other hand, a non-invertible transformation modifies the dynamics of the theory. The reparametrization of Eq. (2.1) falls within this category, thus explaining why the equations of motion are different from those of general relativity [36, 66, 78, 130–138].

Let us now apply mimetic gravity in a cosmological framework. We consider a flat FRW universe (with the  $(+, -, -, -)$  convention)

$$ds^2 = dt^2 - a(t)^2(dx^2 + dy^2 + dz^2). \quad (2.8)$$

Assuming the scalar field to be spatially homogeneous, i.e.  $\phi(t)$ , the constraint (2.2) yields

$$\dot{\phi}^2 = 1, \quad (2.9)$$

which, choosing  $\dot{\phi} > 0$ , upon integration implies

$$\phi = t, \quad (2.10)$$

where the integration constant has been set to zero for convenience. The cosmological equations (2.5) and (2.7) will then read

$$3H^2 = \kappa^2 (\rho + \lambda + V) , \quad (2.11)$$

$$3H^2 + 2\dot{H} = -\kappa^2 (p - V) , \quad (2.12)$$

$$\dot{\lambda} + 3H\lambda + \frac{dV}{d\phi} = 0 , \quad (2.13)$$

with  $H = \dot{a}/a$  the Hubble function and with over-dots denoting differentiation with respect to  $t$ . In the above equations we have considered as usual that the standard-model matter energy-momentum tensor corresponds to a perfect fluid of energy density  $\rho$  and pressure  $p$ . In what follows we will assume a linear equation of state (EoS) for the matter fluid, namely  $p = w\rho$ . Thus, the equations close by the consideration of the matter conservation equation

$$\dot{\rho} + 3H(\rho + p) = 0 . \quad (2.14)$$

Note that Eqs. (2.11)-(2.14) are not independent, since one can obtain any one of (2.12)-(2.14) from the remaining two along with the constraint (2.11) and the condition (2.10). This implies that in order to investigate the dynamics of the system, only an independent subset of these equations needs to be considered. In fact, to derive the dynamical system equations in Sec. 3, we will start from an independent subset of them following the standard procedure commonly used in dynamical systems applications in cosmology [105]. Nevertheless, for the sake of completeness in this section we present all cosmological equations that directly follow from the variation of the mimetic gravity action (2.3).

Note moreover that due to (2.10) the potential  $V(\phi)$  can be considered as a function of  $t$ , namely  $V(t)$ .

We close this section by mentioning that in the case where the potential is absent, equations (2.11) and (2.12) are nothing but the usual cosmological equations with a new non-relativistic matter component given by the Lagrange multiplier  $\lambda$ , which can indeed be used to model dark matter. In particular, from (2.13) we can clearly see that within an FRW background, the energy density of the extra fluid decays with the scale factor as  $a^{-3}$ , precisely as expected for a dust component. Therefore, the construction at hand can mimic cold dark matter on cosmological scales, bypassing the need for an additional dark matter component, that is why it is called ‘‘mimetic gravity’’.

On the other hand, the addition of the potential term  $V(\phi)$  is considered in order to have a mechanism to additionally describe the late-time accelerated expansion (since without a potential this cannot be achieved). When the potential  $V(\phi)$  does not vanish Eq. (2.13) implies that the energy density corresponding to  $\lambda$  is not conserved, due to the interaction with the scalar field  $\phi$ . This implies in particular that instead of following the standard  $a^{-3}$  scaling,  $\lambda$  will evolve with a more general dynamics whenever the derivative of the scalar field potential is not negligible. Note that  $\lambda$  can nevertheless still be identified with the dark matter component at cosmological scales. In fact, the dark matter energy density scales as  $a^{-3}$  only in the absence of an interaction with dark energy, but whenever an interaction is present this is no longer true. This happens in general in every model of interacting dark energy (see for example [139] or the models considered in [140–142]). In our case, when the potential is zero there is no interaction between dark matter and dark energy (since there is no dark energy at all) and dark matter scales as  $a^{-3}$ ; however if the potential is non-zero then an implicit interaction between dark matter (namely  $\lambda$ ) and dark energy (namely  $\phi$ ) is present and the

$a^{-3}$  evolution is modified. Note however that when dark matter dominates then the dark-energy energy density (and thus  $V(\phi)$ ) is effectively zero and thus the interaction does not contribute, implying that standard matter-dominated solutions with  $a^{-3}$  behavior can still appear. On the other hand, when dark energy becomes relevant the evolution of dark matter changes and deviates from the  $a^{-3}$  behavior. This feature explains why scaling solutions with effective equation-of-state parameter different from  $w$  are possible, which is again a standard and well known result from interacting dark energy models for which accelerated scaling solutions can be obtained (see Sec. 6 in [105]).

In summary, in the scenario considered in this work, we have the following sectors: the scalar-field sector which is responsible for dark energy, the mimetic-matter sector which is responsible for dark matter, and the usual standard-model matter which can be either dust matter (in the case of  $w = 0$ ) or radiation (in the case of  $w = 1/3$ ). The various density parameters are defined as usual as

$$\Omega_{de} = \Omega_{\phi} \equiv \frac{\kappa^2 V}{3H^2}, \quad (2.15)$$

$$\Omega_{dm} = \Omega_{\lambda} \equiv \frac{\kappa^2 \lambda}{3H^2}, \quad (2.16)$$

$$\Omega_m \equiv \frac{\kappa^2 \rho}{3H^2}. \quad (2.17)$$

Furthermore, we can define the effective (total) energy density and pressure of the universe as

$$\rho_{\text{eff}} = \rho + \lambda + V, \quad (2.18)$$

$$p_{\text{eff}} = p - V, \quad (2.19)$$

and then the effective equation-of-state parameter as

$$w_{\text{eff}} = \frac{p - V}{\rho + \lambda + V}, \quad (2.20)$$

which is a very useful quantity since it is straightforwardly related to the deceleration parameter  $q$  through

$$q \equiv -1 - \frac{\dot{H}}{H^2} = \frac{1 + 3w_{\text{eff}}}{2}. \quad (2.21)$$

Thus,  $w_{\text{eff}} < -1/3$  implies that the universe is accelerating.

### 3 Dynamical system analysis

In the previous section we presented the cosmological equations of mimetic gravity, in the case of a flat FRW geometry. In this section we are interested in performing the full phase-space analysis, for which one usually introduces suitable dimensionless variables in order to re-write the cosmological equations as an autonomous dynamical system [102–105]. Hence, in order to transform (2.11)–(2.13) into an autonomous system we define

$$\sigma = \frac{\kappa\sqrt{\rho}}{\sqrt{3}H}, \quad x = \frac{\kappa^2\lambda}{3H^2}, \quad y = \frac{\kappa\sqrt{V}}{\sqrt{3}H}, \quad z = -\frac{1}{\kappa V^{3/2}} \frac{dV}{d\phi}. \quad (3.1)$$

Note that  $y$  and  $\sigma$  cannot be negative, while the sign of  $x$  depends on the sign of  $\lambda$ . Using these variables the Friedmann equation (2.11) yields the simple constraint

$$1 = x + y^2 + \sigma^2, \quad (3.2)$$

which can in fact be used to replace  $\sigma$  in terms of  $x$  and  $y$  in the equations that follow, reducing the dimensionality of the autonomous system. Using these auxiliary variables the equations become

$$x' = -3wx^2 - 3x[(w+1)y^2 - w] + \sqrt{3}y^3z, \quad (3.3)$$

$$y' = -\frac{1}{2}y \left[ 3wx + 3(w+1)y^2 - 3(w+1) + \sqrt{3}yz \right], \quad (3.4)$$

$$z' = -\sqrt{3}yz^2 \left( \Gamma - \frac{3}{2} \right), \quad (3.5)$$

where primes denote differentiation with respect to  $N = \ln a$ . Moreover, we have defined

$$\Gamma = \frac{V\ddot{V}}{\dot{V}^2} = \frac{VV_{\phi\phi}}{V_{\phi}^2}, \quad (3.6)$$

where the subscript  $\phi$  denotes differentiation with respect to  $\phi$ , and the last equality arises from (2.10), namely from the fact that  $\phi = t$ . Lastly, the three dimensional phase space of the system (3.3)-(3.5) is given by

$$\Psi = \{(x, y) \in \mathbb{R}^2 \mid -\infty < x \leq 1 - y^2, -\infty < y < \infty\} \times \{z \in \mathbb{R}\}. \quad (3.7)$$

In terms of the auxiliary variables, the various density parameters (2.15)-(2.17) can be expressed as

$$\Omega_m = 1 - x - y^2, \quad \Omega_{\phi} = y^2, \quad \Omega_{\lambda} = x, \quad (3.8)$$

while the effective equation-of-state parameter (2.20) becomes

$$w_{\text{eff}} = w(1 - x - y^2) - y^2, \quad (3.9)$$

with  $w = p/\rho$  the matter equation-of-state parameter.

In order to perform the dynamical analysis we first need to extract the critical points of the system by setting the left hand side of equations (3.3)-(3.5) to zero. Then we perturb the system around these critical points, and thus the type and stability of each point is determined by the eigenvalues of the involved perturbation matrix [102–105]. Since in our model we have the presence of the potential  $V(\phi)$ , in the following subsections we analyze various cases separately.

### 3.1 Mimetic gravity with a general scalar field potential

We start our dynamical analysis keeping the potential general. Observing the definition of  $z$  in (3.1), as well as (3.6), a general potential simply implies that  $\Gamma$  can be written as a function of  $z$ , namely  $\Gamma(z)$ . This encompasses a large variety of scalar field potentials, including the examples analyzed in the next subsections. In the following we use  $z_*$  to denote the solution of the equation  $\Gamma(z) - \frac{3}{2} = 0$  and  $\Gamma_z(z)$  to denote the derivative  $d\Gamma(z)/dz$ . Note that whenever  $y \neq 0$ , the condition  $z = 0$  is not sufficient for making the  $z'$  equation, namely Eq. (3.5), vanish, since a specific scalar field potential could actually induce the expression

$z^2\Gamma(z) \neq 0$  for  $z = 0$ . Hence the two general conditions for attaining  $z' = 0$  are either  $y = 0$  or  $z^2 [\Gamma(z) - \frac{3}{2}] = 0$ .

The physical critical points and curves of critical points for the system of equations (3.3)-(3.5) for a general scalar field potentials are given in Table 1, along with their existence conditions. Additionally, in the same Table we have added the corresponding values of the various density parameters from (3.8), as well as the value of the effective equation-of-state parameter from (3.9). According to  $y$ -definition in (3.1), points with  $y > 0$  correspond to  $H > 0$ , i.e. to expanding universes, while points with  $y < 0$  correspond to  $H < 0$ , i.e. to contracting universes, and thus we respectively add the subscripts + or - to the corresponding points. Furthermore, for each critical point in Table 2 we present the eigenvalues of its involved Jacobian (perturbation) matrix, and the corresponding stability conditions.

Point	$x$	$y$	$z$	Existence	$\Omega_\phi$	$\Omega_\lambda$	$\Omega_m$	$w_{\text{eff}}$
$A_1$	1	0	$z$	Always	0	1	0	0
$A_2$	0	0	$z$	Always	0	0	1	$w$
$A_{3+}$	0	1	0	$z^2\Gamma(z)=0$ for $z=0$	1	0	0	-1
$A_{3-}$	0	-1	0	$z^2\Gamma(z)=0$ for $z=0$	1	0	0	-1
$A_4$	$-\frac{3(1+w)^3}{wz_*^2}$	$\frac{\sqrt{3}(w+1)}{z_*}$	$z_*$	$z_* \neq 0, w \neq 0$	$\frac{3(w+1)^2}{z_*^2}$	$-\frac{3(1+w)^3}{wz_*^2}$	$1 + \frac{3(w+1)^2}{wz_*^2}$	$w$
$A_{5+}$	$1 - \frac{y_+^2}{12}$	$\frac{\sqrt{3}y_+}{6}$	$z_*$	Always	$\frac{y_+^2}{12}$	$1 - \frac{y_+^2}{12}$	0	$-\frac{y_+^2}{12}$
$A_{5-}$	$1 - \frac{y_-^2}{12}$	$\frac{\sqrt{3}y_-}{6}$	$z_*$	Always	$\frac{y_-^2}{12}$	$1 - \frac{y_-^2}{12}$	0	$-\frac{y_-^2}{12}$

**Table 1.** The physical critical points and curves of critical points of the system (3.3)-(3.5), for the case of general potential, and their existence conditions. Additionally, we present the corresponding values of the various density parameters from (3.8), as well as the value of the effective equation-of-state parameter from (3.9). We have defined  $y_\pm = -z_* \pm \sqrt{z_*^2 + 12}$ , with  $z_*$  denoting the solution of the equation  $\Gamma(z) - \frac{3}{2} = 0$ .

Let us summarize the dynamical analysis results for this general potential case.

- $A_1$  is a curve of critical points (each one is obtained by a different value of  $z$ ) which always exists, independently of the potential choice. In these points we have  $\Omega_\lambda = 1$ , and thus  $A_1$  corresponds to a mimetic matter dominated universe, with effective equation of state  $w_{\text{eff}} = 0$  and thus non-accelerating. Since the points of this critical curve behave in general as saddle (see Appendix A) they cannot attract the universe at late times, however the universe can remain in this state for a long period at intermediate times. Thus, critical curve  $A_1$  can very efficiently describe the transient matter-dominated era of the universe history.
- $A_2$  is a curve of critical points, it always exists, independently of the potential choice, and in these states we have  $\Omega_m = 1$ . Hence, they correspond to a universe dominated by the standard-model matter sector, i.e. by dust matter in the case of  $w = 0$  or by radiation in the case where  $w = 1/3$ . Since  $w_{\text{eff}} = w$ , in both cases the universe is non-accelerating. Finally, these points behave as unstable nodes (see Appendix A).
- Critical point  $A_{3+}$  exists for  $z = 0$  and  $z^2\Gamma(z) = 0$ , condition which depends heavily on the potential choice (note that since  $z = 0$  the condition  $z^2 [\Gamma(z) - \frac{3}{2}] = 0$  reduces

Point	$\lambda_1$	$\lambda_2$	$\lambda_3$	Stability
$A_1$	0	$\frac{3}{2}$	$-3w$	non-hyperbolic, behaves as saddle point for $w \neq 0$ behaves as unstable node for $w = 0$
$A_2$	0	$\frac{3}{2}(1+w)$	$3w$	non-hyperbolic, behaves as unstable node
$A_{3+}$	0	-3	$-3(1+w)$	non-hyperbolic, behaves as saddle point for $\Gamma(0) \neq \frac{3}{2}$ behaves as stable for $\Gamma(0) = \frac{3}{2}$ and $\Gamma_z(0) > 0$
$A_{3-}$	0	-3	$-3(1+w)$	non-hyperbolic, behaves as saddle point for $\Gamma(0) \neq \frac{3}{2}$ behaves as stable for $\Gamma(0) = \frac{3}{2}$ and $\Gamma_z(0) < 0$
$A_4$	$\eta_+$	$\eta_-$	$-3(w+1)z_*\Gamma_z(z_*)$	saddle point
$A_{5+}$	$\mu_+$	$\mu_-$	$-\frac{z_*^2}{2}(\sqrt{z_*^2+12}-z_*)\Gamma_z(z_*)$	stable for $\Gamma_z(z_*) > 0$
$A_{5-}$	$\nu_+$	$\nu_-$	$\frac{z_*^2}{2}(\sqrt{z_*^2+12}+z_*)\Gamma_z(z_*)$	stable for $\Gamma_z(z_*) < 0$

**Table 2.** The eigenvalues of the perturbation matrix and the implied stability conditions, for the critical points and curves of critical points of the system (3.3)-(3.5), for the case of general potential. We have defined  $y_{\pm} = -z_* \pm \sqrt{z_*^2 + 12}$ , with  $z_*$  denoting the solution of the equation  $\Gamma(z) - \frac{3}{2} = 0$  and with  $\Gamma_z(z)$  denoting  $d\Gamma(z)/dz$ . Additionally, we have defined  $\eta_{\pm} = \frac{3}{4} \left[ (w-1) \pm \sqrt{\frac{24(1+w)^3}{z_*^2} + (3w+1)^2} \right]$ ,  $\mu_{\pm} = \frac{3}{8} z_* y_{\pm} - \frac{3}{2}(w+6) \pm \frac{\sqrt{2}}{8} \sqrt{(z_*^2 + 12w)(6 - z_* y_{\pm}) - 72w(1-w)}$ , and  $\nu_{\pm} = \frac{3}{8} z_* y_{\pm} - \frac{3}{2}(w+6) \pm \frac{\sqrt{2}}{8} \sqrt{(z_*^2 + 12w)(6 - z_* y_{\pm}) - 72w(1-w)}$ .

to  $z^2\Gamma(z) = 0$ ). It corresponds to a scalar-field (i.e. dark-energy) dominated, expanding de Sitter universe. Since it is non-hyperbolic, with all non vanishing eigenvalues having negative real part, its stability must be determined using the center manifold methods [103]. The relevant analysis of the dynamics near the center manifold is provided in Appendix B and in Table 2 we summarize the results. In particular, point  $A_{3+}$  behaves as saddle for potentials where  $\Gamma(0) \neq \frac{3}{2}$ , while in the cases where  $\Gamma(0) = \frac{3}{2}$  it behaves as stable when  $\Gamma_z(0) > 0$ . The fact that it is dark-energy dominated and stable makes this point a very good candidate for the description of late-time universe.

- Critical point  $A_{3-}$  is the contracting counterpart of  $A_{3+}$ . It corresponds to a scalar-field dominated, contracted universe, which behaves as saddle for potentials where  $\Gamma(0) \neq \frac{3}{2}$ , and as stable in the cases where  $\Gamma(0) = \frac{3}{2}$  with  $\Gamma_z(0) < 0$ .
- Critical point  $A_4$  exists for  $z_* \neq 0$  and  $w \neq 0$ , and its features depend on the specific potential form. It has the interesting property that it can alleviate the cosmic coincidence problem, since in these scaling solutions the dark-energy and dark-matter density parameters can be comparable in magnitude. However since  $w_{\text{eff}} = w$  the universe is non-accelerating for radiation or dust matter fluids. Additionally, since  $\eta_+ > 0$  and  $\eta_- < 0$  its eigenvalues are always of different sign and thus this point behaves always as saddle.
- Critical point  $A_{5+}$  exists always, its features depend on the specific potential form, and it corresponds to an expanding universe (actually point  $A_{3+}$  is a special case of  $A_{5+}$ , namely for potentials that have  $z_* = 0$ ). It can alleviate the coincidence problem, since the dark-energy and dark-matter density parameters can be of the same order, and furthermore for particular values of  $z_*$ , i.e. of the potential form, the universe can be

accelerating. Since the eigenvalues  $\mu_{\pm}$  for  $0 \leq w \leq 1$  are always negative (as can be easily confirmed), its stability depends upon the signature of the eigenvalue  $\lambda_3$ , and thus point  $A_{5+}$  is stable for potentials with  $\Gamma_z(z_*) > 0$ . For the general case  $-1 \leq w \leq 1$ , and with  $\Gamma_z(z_*) > 0$ , the stability region of point  $A_{5+}$  in the  $(w, z_*)$  plane is depicted in the left graph of Fig. 1. The fact that this point can be stable and with features in agreement with observations, makes it a very good candidate for the description of the late-time universe.

- Critical point  $A_{5-}$  is the contracting counterpart of  $A_{5+}$  (again,  $A_{3-}$  is a special case of  $A_{5-}$ , for potentials that have  $z_* = 0$ ). For  $0 \leq w \leq 1$  it is stable when  $\Gamma_z(z_*) < 0$ , while for the general case  $-1 \leq w \leq 1$ , and with  $\Gamma_z(z_*) < 0$ , its stability region in the  $(w, z_*)$  plane is depicted in the right graph of Fig. 1.

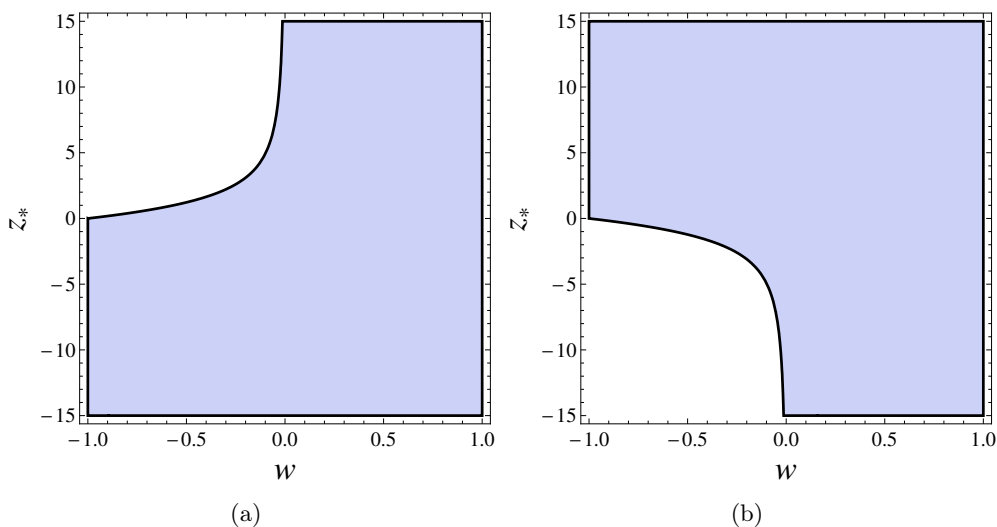


**Figure 1.** Left graph: The shaded regions mark the stability region of point  $A_{5+}$  in the  $(w, z_*)$  plane, when  $\Gamma_z(z_*) > 0$ . Right graph: The stability region of point  $A_{5-}$  in the  $(w, z_*)$  plane, when  $\Gamma_z(z_*) < 0$ .

The above general dynamical analysis reveals that, irrespectively of the form of the scalar field potential, the cosmological behavior of mimetic gravity will always admit both matter dominated solutions (curves  $A_1$  and  $A_2$ ) and dark-energy dominated solutions mimicking a cosmological constant behavior (points  $A_{3+}$ ). Moreover, the phase space presents scaling solutions (points  $A_4$  and  $A_{5+}$ ) too, in which the matter and dark-energy density parameters are of the same order and thus they can offer an alleviation to the coincidence problem, where the exact behavior of the accelerating expansion depends on the specific potential form.

In order to proceed from the above general examination to a more precise analysis we need to specify the potential  $V(\phi)$ . In the following three subsections we investigate some well-known scalar field potentials separately.

### 3.2 Mimetic gravity with an inverse square potential

Let us start with the study of the inverse square scalar-field potential, namely we consider

$$V(\phi) = \alpha\phi^{-2}, \quad (3.10)$$

with  $\alpha > 0$  the potential parameter. This potential form has the special property that, through (3.6), it yields  $\Gamma = 3/2$  and consequently  $z' = 0$  from Eq. (3.5). This implies that  $z_*$  in Tab. 1 can be treated as an arbitrary constant. From the definition of  $z$  in Eq. (3.1), we deduce that

$$z = \frac{2}{\kappa\sqrt{\alpha}}, \quad (3.11)$$

and thus  $z_*$  is actually related to  $\alpha$ . The fact that the variable  $z$  has a constant value implies that in this special potential case the autonomous system (3.3)–(3.5) becomes two-dimensional.

The critical points of the system and their properties for this potential case can be extracted from the general Tables 1 and 2, through the replacement  $z_* = \frac{2}{\kappa\sqrt{\alpha}}$ . Hence, in Table 3 we present the physical critical points of the system (3.3)–(3.5), the corresponding values of the various density parameters from (3.8), as well as the value of the effective equation-of-state parameter from (3.9). Additionally, in Table 4 we list the eigenvalues of the perturbation matrix and the implied stability conditions.

Point	$x$	$y$	Existence	$\Omega_\phi$	$\Omega_\lambda$	$\Omega_m$	$w_{\text{eff}}$
$A_1$	1	0	Always	0	1	0	0
$A_2$	0	0	Always	0	0	1	$w$
$A_4$	$-\frac{3\kappa^2\alpha(1+w)^3}{4w}$	$\frac{\sqrt{3\alpha}\kappa(w+1)}{2}$	$w \neq 0$	$\frac{3\kappa^2\alpha(1+w)^2}{4}$	$-\frac{3\kappa^2\alpha(1+w)^3}{4w}$	$1 + \frac{3\kappa^2\alpha(1+w)^2}{4w}$	$w$
$A_{5+}$	$1 - \frac{y_+^2}{12}$	$\frac{\sqrt{3}y_+}{6}$	$\alpha \neq 0$	$\frac{y_+^2}{12}$	$1 - \frac{y_+^2}{12}$	0	$-\frac{y_+^2}{12}$
$A_{5-}$	$1 - \frac{y_-^2}{12}$	$\frac{\sqrt{3}y_-}{6}$	$\alpha \neq 0$	$\frac{y_-^2}{12}$	$1 - \frac{y_-^2}{12}$	0	$-\frac{y_-^2}{12}$

**Table 3.** The physical critical points of the system (3.3)–(3.5), for the case of inverse square scalar-field potential  $V = \alpha\phi^{-2}$ , and their existence conditions. Additionally, we present the corresponding values of the various density parameters from (3.8), as well as the value of the effective equation-of-state parameter from (3.9). We have defined  $y_\pm = -\frac{2}{\kappa\sqrt{\alpha}} \pm \sqrt{\frac{4}{\kappa^2\alpha} + 12}$ .

The critical curves  $A_1$  and  $A_2$  of the general case have now become individual critical points. Point  $A_1$  corresponds to a mimetic matter dominated, non-accelerating universe, which is a saddle and thus can describe the matter-dominated era of the universe history at intermediate times. Point  $A_2$  corresponds to a non-accelerating universe dominated by the standard-model matter sector (by dust matter in the case of  $w = 0$  or by radiation in the case where  $w = 1/3$ ), and is unstable. Moreover, the critical points  $A_{3\pm}$  of the general case do not exist for this specific potential, since they require  $z = 0$ . Furthermore, critical point  $A_4$  exists for  $w \neq 0$ , it is always saddle, and it corresponds to a non-accelerating universe with scaling behavior, which can alleviate the coincidence problem.

Critical point  $A_{5+}$  corresponds to a universe with scaling behavior, and thus can alleviate the coincidence problem. Additionally, since  $w_{\text{eff}} = -\frac{y_+^2}{12}$  we deduce that we obtain acceleration for  $-y_+^2/12 < -1/3$ , i.e. for  $\kappa^2\alpha > 1$ . Since the eigenvalues  $\mu_\pm$  for  $0 \leq w \leq 1$  are always negative (as can be easily confirmed), this point is always stable and therefore can correspond the late-time evolution of the universe. It is the most interesting solution of the scenario at hand. Finally, point  $A_{5-}$  is its contracting counterpart. Let us mention here that for a given potential parameter both  $A_{5+}$  and  $A_{5-}$  are stable, however since  $y = 0$  separates

Point	$\lambda_1$	$\lambda_2$	Stability
$A_1$	$\frac{3}{2}$	$-3w$	saddle
$A_2$	$\frac{3}{2}(1+w)$	$3w$	unstable
$A_4$	$\eta_+$	$\eta_-$	saddle
$A_{5+}$	$\mu_+$	$\mu_-$	stable for orbits with $y > 0$
$A_{5-}$	$\nu_+$	$\nu_-$	stable for orbits with $y < 0$

**Table 4.** The eigenvalues of the perturbation matrix and the implied stability conditions, for the critical points of the system (3.3)-(3.5), for the case of inverse square scalar-field potential  $V = \alpha\phi^{-2}$ .

We have defined  $y_{\pm} = -\frac{2}{\kappa\sqrt{\alpha}} \pm \sqrt{\frac{4}{\kappa^2\alpha} + 12}$ ,  $\eta_{\pm} = \frac{3}{4} \left[ (w-1) \pm \sqrt{12\kappa^2\alpha(1+w)^3 + (3w+1)^2} \right]$ ,  $\mu_{\pm} = \frac{3}{4} \frac{y_{\pm}}{\kappa\sqrt{\alpha}} - \frac{3}{2}(w+6) \pm \frac{1}{2} \sqrt{(\frac{1}{\kappa^2\alpha} + 3w)(3 - \frac{y_{\pm}}{\kappa\sqrt{\alpha}}) - 9w(1-w)}$ ,  $\nu_{\pm} = \frac{3}{4} \frac{y_{\pm}}{\kappa\sqrt{\alpha}} - \frac{3}{2}(w+6) \pm \frac{1}{2} \sqrt{(\frac{1}{\kappa^2\alpha} + 3w)(3 - \frac{y_{\pm}}{\kappa\sqrt{\alpha}}) - 9w(1-w)}$ .

the phase space to two disconnected parts, orbits with  $y > 0$  initially, i.e. expanding universes, will always remain in the upper half of the phase space and thus they will be attracted by  $A_{5+}$  at late times, while orbits with  $y < 0$  initially, i.e. contracting universes, will always remain in the lower part of the phase space and thus they will be attracted by  $A_{5-}$ .

In order to present the above features in a more transparent way, we evolve the autonomous system numerically and in Fig. 2 we depict the resulting two-dimensional phase-space behavior for two choices of  $w$ , namely for dust matter with  $w = 0$  (left graph) and for radiation with  $w = 1/3$  (right graph).

For the dust matter case of the left graph of Fig. 2, we remind that  $\Omega_m$  characterizes the non-relativistic baryonic component, while  $\Omega_{\lambda}$  constitutes the dark matter sector and  $\Omega_{\phi}$  the dark energy sector. Note that as we discuss in Appendix A, for  $w = 0$  the whole  $x$ -axis becomes a critical line. As we observe, we do verify the theoretical prediction that  $y = 0$  separates the phase space to two disconnected parts, i.e. to  $y > 0$ , which corresponds to expanding universe, and to  $y < 0$ , which corresponds to contracting universe. Hence, given any choice of parameters and initial conditions, an expanding universe evolves from a matter dominated universe (line  $A_1$  or  $A_2$ ) towards the scaling universe  $A_{5+}$ , which for the specific choice  $\alpha = 9/\kappa^2$  of the figure it is also accelerating. This cosmological behavior is in agreement with observations. On the other hand, an initially contracting universe will result to the contracting late-time attractor  $A_{5-}$ .

For the radiation case depicted in the right graph of Fig. 2, we remind that since  $w = 1/3$  then  $\Omega_m$  characterizes the radiation component, while  $\Omega_{\lambda}$  constitutes the dark matter sector and  $\Omega_{\phi}$  the dark energy sector. In this case, points  $A_1$  or  $A_2$  are isolated critical points, with the first corresponding to dark-matter domination (since  $\Omega_{\lambda} = 1$ ) while the second to radiation domination (since  $\Omega_m = 1$ ). This scenario exhibits a very interesting behavior: the universe may start from the unstable point  $A_2$ , come close to the saddle point  $A_1$  and remain around it for sufficiently long time, and finally result to the scaling (and accelerating for  $\alpha = 9/\kappa^2$ ) universe  $A_{5+}$ . Thus, we obtain the required thermal history of the universe, namely the successive sequence of radiation, matter and acceleration eras.

The above features are alternatively evident in Fig. 3, where we plot the evolutions of

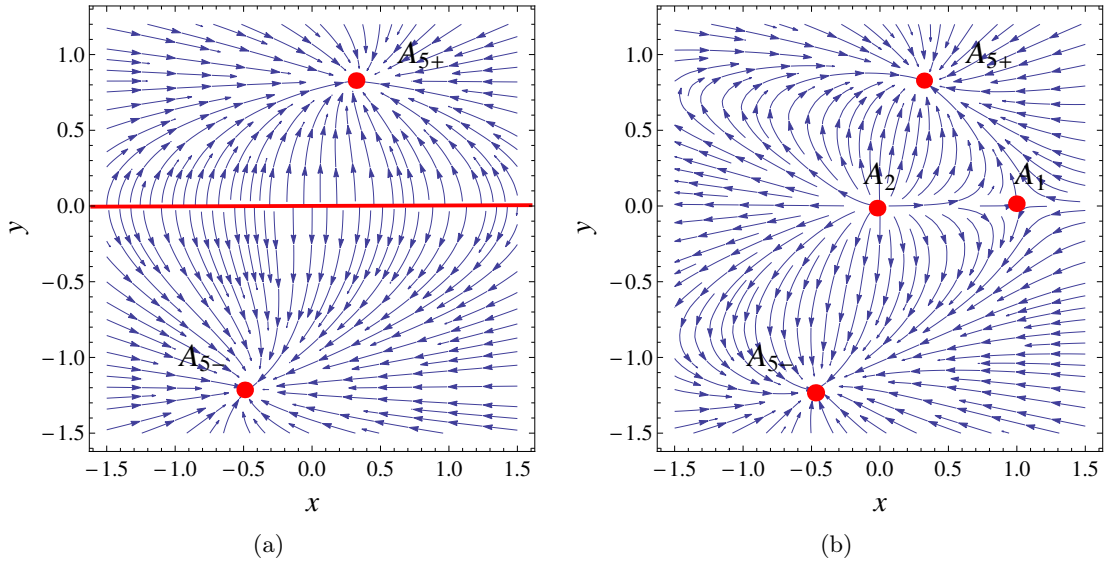


**Figure 2.** The phase-space behavior of the system (3.3)-(3.4), for the case of inverse square scalar-field potential  $V = \alpha\phi^{-2}$ , with the choice  $\alpha = 9/\kappa^2$ , for  $w = 0$  (left graph) and  $w = 1/3$  (right graph), respectively. As we explain in the text, orbits with  $y > 0$  initially, i.e. expanding universes, will result to the (accelerating for this  $\alpha$  value) scaling solution  $A_{5+}$ , while orbits with  $y < 0$  initially, i.e. contracting universes, will result to the contracting counterpart  $A_{5-}$ .

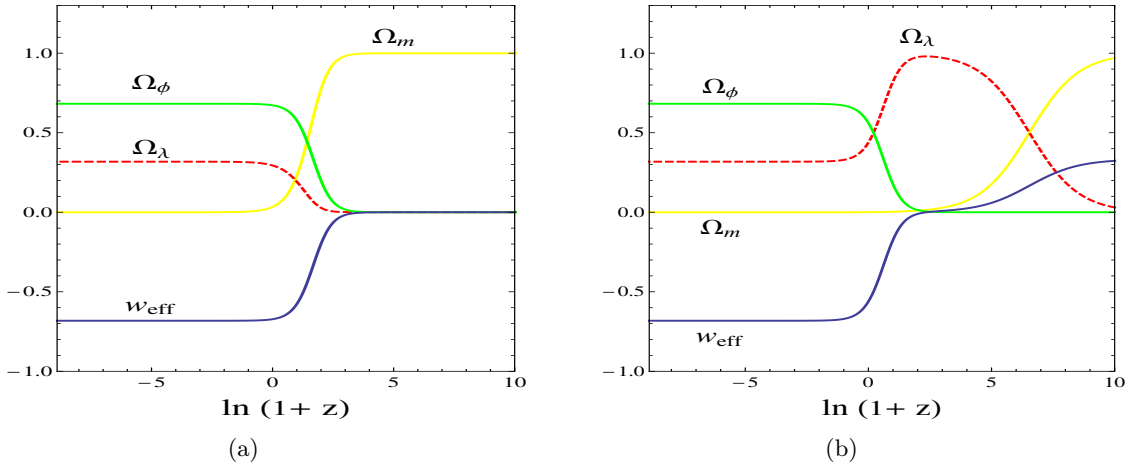


**Figure 3.** The evolution of the density parameters  $\Omega_m$ ,  $\Omega_\phi$ ,  $\Omega_\lambda$ , as well as of the effective equation-of-state parameter  $w_{\text{eff}}$ , as functions of the redshift, for the case of inverse square scalar-field potential  $V = \alpha\phi^{-2}$ , with the choice  $\alpha = 9/\kappa^2$ , for  $w = 0$  (left graph) and  $w = 1/3$  (right graph), respectively.

the various density parameters, as well as of the effective equation-of-state parameter  $w_{\text{eff}}$ . For convenience, as independent variable we use the redshift  $z = a_0/a - 1$  (with  $a_0 = 1$  the present scale factor), and thus as usual  $z = 0$  corresponds to the present time while  $z \rightarrow -1$  corresponds to the infinite future.

For the dust case in the left graph of Fig. 3 we do observe the aforementioned behavior, namely the universe transits from a matter to an acceleration era at late times, and moreover the dark matter and dark energy density parameters remain, respectively, around 0.3 and 0.7

for ever after, therefore offering an alleviation to the coincidence problem.

For the radiation case of the right graph of Fig. 3 we can see that at early times the universe is radiation dominated, then it transits to dark matter domination, and finally it results to dark energy domination. As before, the universe results in a scaling accelerating solution, where the dark matter and dark energy density parameters remain around 0.3 and 0.7 respectively for ever, offering an alleviation to the coincidence problem. Furthermore, the early-time behavior is in agreement with observations, since the past attractor is described by a radiation dominated solution. We stress that this is not the case for simpler scalar-field models of dark energy, notably quintessence, since in those models the past attractor of the system is always a stiff-matter solution dominated by the kinetic energy of the scalar field [106, 144].

In summary, as we can see, mimetic gravity with an inverse square potential can describe very efficiently the expansion history of the universe, starting from early radiation domination, transiting to the matter era at intermediate times, and resulting to late-time acceleration, offering also an alleviation to the coincidence problem.

### 3.3 Mimetic gravity with a power-law or exponential potential

In this subsection we investigate the cosmology of mimetic gravity with a power-law or an exponential scalar-field potential, namely we consider

$$V(\phi) \propto \phi^n, \quad (3.12)$$

with  $n \neq -2$  (the case  $n = 2$  was analyzed in the previous subsection), or

$$V(\phi) \propto e^{\alpha\phi}, \quad (3.13)$$

with  $\alpha$  the model parameter. For both these potential cases  $\Gamma$  is constant, and in particular  $\Gamma = (n - 1)/n$  for the power-law potential, while  $\Gamma = 1$  for the exponential potential. Hence in the following we perform a general analysis of Eqs. (3.3)-(3.5) considering  $\Gamma = \text{const.} \neq 3/2$  (actually  $\Gamma = 3/2$  only for the inverse square potential case, and that is why we analyzed it separately in the previous subsection).

The critical points and their features will arise from the results of the general potential case of Tables 1 and 2, substituting  $\Gamma = \text{const.} \neq 3/2$ . In this case the equation  $\Gamma(z) - \frac{3}{2} = 0$  does not have any solution  $z_*$ , and thus critical points  $A_4$  and  $A_{5\pm}$  do not exist.

Since the curves of critical points  $A_1$  and  $A_2$  are independent from the choice of the potential, their cosmological properties that were discussed in the general potential case of subsection 3.1 will hold here too. In particular, saddle points  $A_1$  correspond to a non-accelerating mimetic matter dominated universe, while unstable points  $A_2$  correspond to a non-accelerating universe dominated by the standard-model matter sector, i.e. by dust matter in the case of  $w = 0$  or by radiation in the case where  $w = 1/3$ .

Furthermore, since now the system (3.3)-(3.5) is invariant under the transformation  $(y, z) \rightarrow (-y, -z)$ , the stability features of points  $A_{3+}$  and  $A_{3-}$  are the same. Since  $\Gamma = \text{const.} \neq 3/2$ , from the analysis performed in Sec. 3.1, and by employing center manifold techniques, we conclude that in the present case both critical points  $A_{3\pm}$  are saddle.  $A_{3+}$  corresponds to a dark-energy dominated, expanding de Sitter universe, while  $A_{3-}$  is its contracting counterpart.

Hence, for these particular choices of  $V(\phi)$  there is no late time attractor in the finite regime. The attractor exists at infinity, and its exact investigation requires to apply the

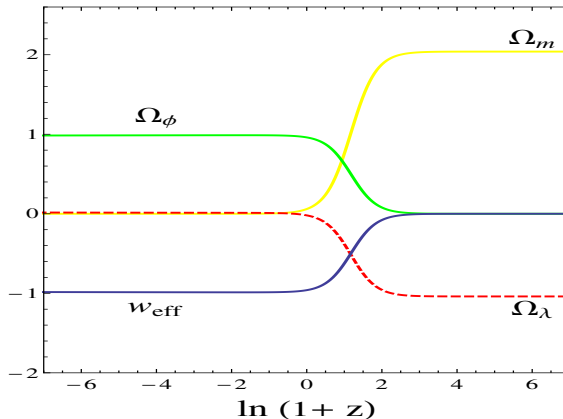


**Figure 4.** The evolution of the density parameters  $\Omega_m$ ,  $\Omega_\phi$ ,  $\Omega_\lambda$ , as well as of the effective equation-of-state parameter  $w_{\text{eff}}$ , as functions of the redshift, for the case of power-law scalar-field potential  $V(\phi) \propto \phi^n$ , with the choice  $n = 3$ , for  $w = 0$ .

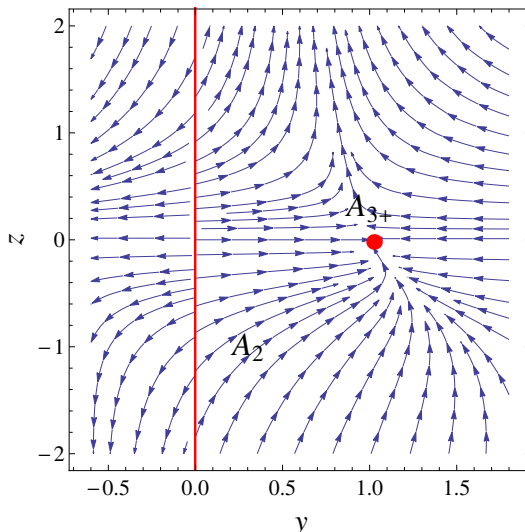


**Figure 5.** The phase-space behavior of the system (3.3)-(3.4) projected on the  $x = 0$  plane, for the case of power-law scalar-field potential  $V(\phi) \propto \phi^n$ , with the choice  $n = 3$  and for  $w = 0$ . The universe starts from the matter-dominated critical line  $A_2$ , resulting in the dark-energy dominated saddle de Sitter point  $A_{3+}$ .

Poincaré central projection method [103]. However, since this analytical investigation lies beyond the scope of the present work, we examine the cosmological behavior numerically. In Fig. 4 we depict the evolutions of the various density parameters, as well as the effective equation-of-state parameter  $w_{\text{eff}}$ , as functions of the redshift. As we observe, the universe starts evolving from a matter dominated phase, and then it transits to the dark-energy dominated phase, resulting finally to the de Sitter point  $A_{3+}$ . Nevertheless, since the de Sitter phase is not stable but saddle, the universe will remain close to that for a finite time interval. In order to see this behavior more transparently, in Fig. 5 we present the corresponding phase-space behavior projected on the  $x = 0$  plane, where we also see that the universe starts from the matter-dominated critical line  $A_2$ , resulting in the dark-energy dominated de Sitter

point  $A_{3+}$ .

Note that in Fig. 4 the relative energy densities  $\Omega_m$  and  $\Omega_\lambda$  are not constrained in the interval  $[-1, 1]$ , as one would expect. This feature usually arises in cosmological models where an interaction between the matter component sourcing the cosmological equations is present (see e.g. [145]) and it is related to a certain ambiguity in defining the relative energy densities that is present in this class of models [146]. Since in our mimetic model the fields  $\phi$  and  $\lambda$  can be interpreted as effectively interacting quantities (cf. Eq. (2.13)), then it is not surprising that the relative energy densities  $\Omega_m$  and  $\Omega_\lambda$  can acquire values outside the range  $[-1, 1]$ .

### 3.4 Mimetic gravity with $V(\phi) \propto (1 + \beta\phi^2)^{-2}$

In this subsection we consider the scalar potential [27]

$$V(\phi) = \alpha(1 + \beta\phi^2)^{-2}, \quad (3.14)$$

where  $\alpha$  and  $\beta$  are two parameters of suitable dimensions. For this potential the variable  $z$  defined in (3.1) becomes

$$z = \frac{4\beta\phi}{\sqrt{\alpha\kappa}}, \quad (3.15)$$

implying that  $\Gamma$  in (3.6) can be written as

$$\Gamma = \frac{5}{4} \left( 1 + \frac{\xi}{5z^2} \right), \quad (3.16)$$

where we have defined

$$\xi = -\frac{16\beta}{\alpha\kappa^2}. \quad (3.17)$$

The critical points and their features will arise from the results of the general potential case of Tables 1 and 2, substituting  $\Gamma(z)$  from (3.16). In this case, Eq. (3.5) becomes

$$z' = \frac{\sqrt{3}}{4} y (z^2 - \xi), \quad (3.18)$$

and thus we have two solutions  $z_* = \pm\sqrt{\xi}$ . Hence, for this potential, points  $A_{3\pm}$  do not exist, while points  $A_4$ ,  $A_{5\pm}$  exist for  $\xi > 0$ . Critical point  $A_4$  is saddle, since the eigenvalues  $\eta_+$  and  $\eta_-$  are of opposite signs. Additionally, since there are two solutions  $z_* = \pm\sqrt{\xi}$ , there are then two copies for each of the points  $A_{5\pm}$ . We denote these points as  $A_{5\pm}^\pm$ , with the upper sign corresponding to one of the two solutions  $z_* = \pm\sqrt{\xi}$ . For  $z_* = \sqrt{\xi}$  critical point  $A_{5-}^+$  is stable, but point  $A_{5+}^+$  is saddle (as  $\Gamma_z(\sqrt{\xi}) < 0$ ). On the other hand, for  $z_* = -\sqrt{\xi}$  point  $A_{5+}^-$  is stable, while point  $A_{5-}^-$  is saddle (as  $\Gamma_z(-\sqrt{\xi}) > 0$ ). Finally, for  $\xi < 0$  only the critical lines  $A_1$  and  $A_2$  exist and hence there is no finite late-time attractor in this case.

Point  $A_{5+}^-$  corresponds to a phantom dark-energy dominated expanding solution, while point  $A_{5+}^+$  describes a scaling solution that can be accelerating. In particular, the effective equation-of-state parameter for  $A_{5+}^-$  always satisfies  $w_{\text{eff}} < -1$ , while for  $A_{5+}^+$  it always satisfies  $-1 < w_{\text{eff}} < 0$ , which provides accelerated expansion as long as  $w_{\text{eff}} < -1/3$ .

In Fig. 6 we present the three-dimensional phase space of the system (3.3)-(3.5), for the potential (3.14) (with  $\xi > 0$ ). Here the selected trajectories start evolving from a matter domination solution corresponding to the critical plane  $A_2$  towards the accelerating phantom scaling solution  $A_{5+}^-$ , and in some cases they pass also through the intermediate long lasting accelerating scaling solution  $A_{5+}^+$ . Additionally, one may also have a similar behavior in the

contracting counterparts, namely the contracting universe starts from the matter dominated solution, evolving towards  $A_{5-}^-$ , and in some case passing also through the intermediate long lasting scaling solution  $A_{5-}^+$ .

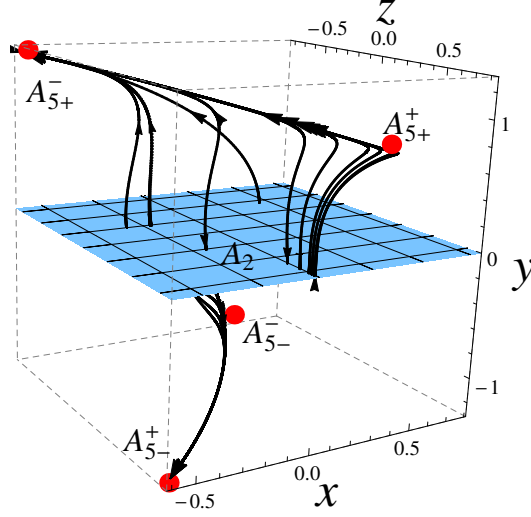


**Figure 6.** Selected phase trajectories of the system (3.3)-(3.4) for the potential  $V(\phi) = \alpha(1 + \beta\phi^2)^{-2}$ , with  $\xi = -\frac{16\beta}{\alpha\kappa^2} = 0.3$  and for  $w = 0$ . The expanding universe starts from a matter domination solution corresponding to the critical plane  $A_2$ , moving towards the accelerating phantom scaling solution  $A_{5+}^-$ , and in some cases it also passes through the intermediate long lasting accelerating scaling solution  $A_{5+}^+$ . Additionally, one may also have a similar behavior in the contracting counterparts, namely the contracting universe starts from the matter dominated solution, evolving towards  $A_{5-}^-$ , and in some case passing also through the intermediate long lasting scaling solution  $A_{5-}^+$ .

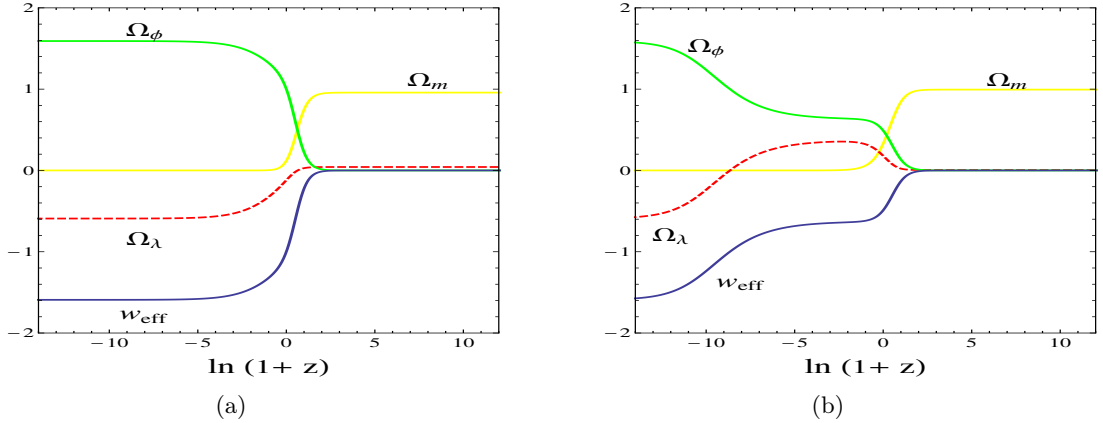


**Figure 7.** The evolution of the density parameters  $\Omega_m$ ,  $\Omega_\phi$ ,  $\Omega_\lambda$ , as well as of the effective equation-of-state parameter  $w_{\text{eff}}$ , as functions of the redshift, for the case of potential  $V(\phi) = \alpha(1 + \beta\phi^2)^{-2}$ , with  $\xi = -\frac{16\beta}{\alpha\kappa^2} = 0.3$  and for  $w = 0$ . The left and right graphs correspond to different initial conditions.

In order to see these features in an alternative way, in Fig. 7 we depict the evolution of the various density parameters, as well as of the effective equation-of-state parameter  $w_{\text{eff}}$ , as functions of the redshift, for two choices of the initial conditions. Qualitatively

there are thus two possible cosmic evolutions. The first one is depicted in the left panel of Fig. 7, where a transition from matter domination to phantom behavior is achieved. This is provided by trajectories directly connecting the critical plane  $A_2$  with point  $A_{5+}^-$ . The second evolution class is depicted in the right panel of Fig. 7, where after matter domination a long lasting finite period of quintessence-like acceleration is attained before a transition to the final phantom domination happens. This scenario is very interesting because the unstable accelerating scaling solution can be used to alleviate the cosmic coincidence problem. The future destiny of the universe is however a phantom dominated solution, which could lead to a Big Rip singularity in a finite time. Note that a current phantom-like dark energy scenario appears more plausible than a quintessence-like in light of the reported preference for the normal neutrino mass hierarchy from cosmological data [147, 148]. Note also that in Fig. 7 the relative energy densities are again not constrained in the interval  $[-1, 1]$ . As mentioned above this is an issue related to cosmological models where an effective interaction between the components sourcing the field equations is present [145, 146].

## 4 Cosmological implications

In the previous section we performed a detailed phase-space and stability analysis for the scenario of mimetic gravity with the inclusion of a scalar-field potential. In this section we discuss the physical implications of the analysis. The cosmological dynamics of the mimetic gravity exhibits a very rich phenomenology, including for example matter to dark energy transitions, phantom behavior and accelerated scaling solutions. Apart from being in agreement with observations, these solutions can be in fact used to alleviate some of the problems afflicting modern cosmology, such as the cosmic coincidence problem.

In the case of a general potential, and irrespectively of its form, the cosmological behavior of mimetic gravity will always admit both matter dominated solutions, and dark-energy dominated solutions mimicking a cosmological constant, or quintessence-like, or phantom-like behavior. Furthermore, the phase space presents scaling solutions too, in which the matter and dark-energy density parameters are of the same order and thus they can offer an alleviation to the coincidence problem. Hence, one can easily describe the universe history in agreement with observations, namely the successive sequence of radiation, matter, and dark-energy eras.

Specifying the potential to the case of an inverse square form, not only yields accelerating scaling solutions, which can be used to solve the cosmic coincidence problem, but it also provides an early time matter-dominated state, which in the case of  $w = 1/3$  can be used to well characterize the radiation era, while for  $w = 0$  it corresponds to the dust matter epoch. In fact, choosing proper initial conditions of the universe, the cosmic dynamics of mimetic gravity with this potential, and with suitable parameter choices, will lead to a universe which starts from a radiation phase, it enters into a matter-dominated epoch, and then it transits to a scaling solution with  $w_{\text{eff}} \simeq -0.7$ , in agreement with observations. This scenario is thus not only mathematically simple to be analyzed (it yields a two-dimensional dynamical system), but it is also phenomenologically very powerful.

The cosmological scenario is different for mimetic gravity with an exponential or power-law potential. In this case there is no accelerating scaling solution and there is no finite final attractor in the phase space. The observed transition from matter to dark energy domination can still however be correctly described since a finite period of cosmological constant behavior can still be attained after a long-lasting matter solution. An expansion history similar to

$\Lambda$ CDM cosmology can thus still be achieved, although in the far future the universe may be lead to a sudden Big Rip singularity.

In the case of the potential  $V(\phi) = \alpha(1 + \beta\phi^2)^{-2}$ , we found two possible qualitative cosmic evolutions. In the first one we obtained a matter-dominated early time solution, followed by a phantom-like late-time accelerated phase. In the second class of cosmic evolutions we found that between the early-time matter domination and the future phantom behavior, there is a long lasting finite period described by an accelerating scaling solution, which can actually be used to alleviate the cosmic coincidence problem. Choosing suitable model parameters one can also obtain  $w_{\text{eff}} \simeq -0.7$  during the scaling regime, in agreement with observations [4]. This model can thus both alleviate the cosmic coincidence problem and provide a well-behaved early-time dynamics, similarly to the inverse square potential. It nevertheless leads to a different cosmological scenario where the present state of the universe is described by an accelerating scaling solution, but in the future a transition to a phantom regime will happen and the universe may approach a Big Rip singularity.

## 5 Conclusions

Mimetic gravity has emerged as an interesting alternative to general relativity. Within this theory, the conformal degree of freedom of gravity is isolated in a covariant way through a singular disformal transformation: the resulting dynamics changes and an effective dark matter component appears on cosmological scales. Various works have previously investigated background cosmological solutions in mimetic gravity, finding that appropriate choices of the potential for the mimetic field lead to appealing cosmological solutions, which can reproduce expansion histories in agreement with observational data without the need for additional dark matter or dark energy fluids.

In this work we have performed a dynamical-systems analysis of mimetic gravity, which has allowed us to study the cosmological dynamics of the theory. We have focused on both general potentials for the mimetic field, as well as on a set of well-motivated specific choices. From the point of view of the expansionary history, our analysis suggests that the potential whose solutions are most appealing is the inverse square potential. The corresponding solutions possess an early-time radiation phase, followed successively by matter era and late-time accelerating scaling solution, which can alleviate the coincidence problem. We mention that this alleviation of the coincidence problem is obtained without imposing an interaction between dark-matter and dark-energy sectors by hand, as it is the usual approach [140], but it arises from the scenario of mimetic gravity itself. Therefore, with this choice of potential, mimetic gravity is in agreement with observations, and it provides the correct phenomenology at early times, as opposed to simpler scalar-field models of dark energy where a stiff-matter dominated early-time solution is usually attained. Moreover, it should be remarked that the inverse square potential is also very well motivated from a high-energy ultraviolet completion point of view, aside from being renormalizable, which lends even more to the attractiveness of the model.

In summary, mimetic gravity with an inverse square potential yields:

- A unified description of both dark matter and dark energy with a single scalar field;
- A well behaved early-time phenomenology;
- The successive sequence of radiation, matter, and dark-energy eras, with transitions in agreement with observations;

- Late time accelerated scaling solutions that can alleviate the cosmic coincidence problem;
- A scalar-field potential with interesting theoretical features.

In conclusion in our work we have shown that the cosmological dynamics of mimetic gravity renders the theory a viable and interesting candidate to explain the universe’s history. At the same time, it is important and timely to go beyond the background analysis and analyze and understand structure formation within this scenario, as well as provide a full Markov Chain Monte Carlo analysis, comparing the model with observational data. It will also be important to confirm or discard the raised issues concerning instabilities, in order to ascertain whether or not the theory of mimetic gravity is really viable. We leave these issues to future projects.

## Acknowledgments

J.D. acknowledges the support of Associate program of IUCAA. N.T. acknowledges partial support from the Labex P2IO and an Enhanced Eurotalents Fellowship. S.V. acknowledges support by the Vetenskapsrådet (Swedish Research Council) through contract No. 638-2013-8993 and the Oskar Klein Centre for Cosmoparticle Physics. N.T. and S.V. wish to thank the NORDITA cosmology program “Advances in theoretical cosmology in light of data” and in particular Martina Gerbino, scientific organizer for the first week of the program, where discussions leading to this work were conducted. E.N.S. desires to thank Institut de Physique Théorique, Université Paris-Saclay and Laboratoire de Physique Théorique, Univ. Paris-Sud, Université Paris-Saclay, for the hospitality during the last stages of this project. This article is based upon work from COST Action “Cosmology and Astrophysics Network for Theoretical Advances and Training Actions”, supported by COST (European Cooperation in Science and Technology).

## A Appendix: stability analysis for $A_1, A_2$

In this Appendix we analyze the stability of the curves of critical points  $A_1$  and  $A_2$  presented in Table 1. As it is known a set of non-isolated critical points with  $N$  vanishing eigenvalues is called “normally hyperbolic set of dimension  $N$ ”. The  $N$ -dimensional eigenspace spanned by the eigenvectors corresponding to the vanishing eigenvalues (eigenvalues with vanishing real part) determine the direction of the critical set. The stability of this set is therefore determined by the behavior of trajectories on the eigenspace spanned by eigenvectors corresponding to the non-vanishing eigenvalues (eigenvalues with non-vanishing real part). Thus, the stability depends on the signature of nonvanishing eigenvalues.

In order to properly determine the stability behavior of sets  $A_1$  and  $A_2$ , we shall examine the  $w \neq 0$  and  $w = 0$  separately.

### A.1 Case: $w \neq 0$

In this case curves  $A_1$  and  $A_2$  are normally hyperbolic sets of critical points. Hence, looking from the signature of non-vanishing eigenvalues, we can conclude that  $A_1$  behaves as a saddle and  $A_2$  behaves as an unstable node.

## A.2 Case: $w = 0$

In this case the stability depends on the value of  $\Gamma(z)$ :

- For potentials with  $\Gamma(z) = \frac{3}{2}$ , the  $x$ -axis becomes a critical line. Thus, curves  $A_1, A_2$  are replaced by a single critical line, namely the  $x$ -axis. Since the stability matrix of the  $x$ -axis has eigenvalues  $(\frac{3}{2}, 0)$  it is normally hyperbolic. Hence, the  $x$ -axis behaves as an unstable node.
- For potential with  $\Gamma(z) \neq \frac{3}{2}$ , the plane  $y = 0$  becomes a critical plane. Therefore, curves  $A_1, A_2$  are replaced by this plane. The plane  $y = 0$  is normally hyperbolic of dimension 2, with eigenvalues  $(\frac{3}{2}, 0, 0)$ . Thus, the stability depends on the signature of non-vanishing eigenvalues. Hence, the plane  $y = 0$  is behaving as an unstable node.

We close this Appendix by mentioning that we have indeed verified that in the above cases the center manifold is actually the critical set itself. Hence, the behavior of trajectories on the center manifold cannot provide the stability of the critical set. Nevertheless, the stability is completely determined by the behavior of trajectories on the eigenspace, spanned by eigenvectors corresponding to the remaining non-vanishing eigenvalues. Thus, the stability depends on the signature of the non-vanishing eigenvalues.

The stability results of curves  $A_1$  and  $A_2$  are summarized in Table 2.

## B Appendix: stability analysis for $A_{3\pm}$

In this Appendix, we apply the center manifold method [103] in order to study the stability of the non-hyperbolic points  $A_{3\pm}$  presented in Table 1. We first translate the point  $A_{3+}(0, 1, 0)$  to the origin via the transformation  $x \rightarrow x, y \rightarrow y + 1, z \rightarrow z$ . We then introduce a new set of variables  $(X, Y, Z)$ , defined in terms of the original set of variables  $(x, y, z)$  as

$$\begin{pmatrix} X \\ Y \\ Z \end{pmatrix} = \begin{pmatrix} -2 & 0 & \frac{1}{\sqrt{3}} \\ 1 & 1 & -\frac{\sqrt{3}}{6} \\ 0 & 0 & 1 \end{pmatrix} \begin{pmatrix} x \\ y \\ z \end{pmatrix}.$$

In terms of these new set of variables, the system of equations can be re-written as

$$\begin{pmatrix} X' \\ Y' \\ Z' \end{pmatrix} = \begin{pmatrix} -3 & 0 & 0 \\ 0 & -3(w+1) & 0 \\ 0 & 0 & 0 \end{pmatrix} \begin{pmatrix} X \\ Y \\ Z \end{pmatrix} + \begin{pmatrix} g_1 \\ g_2 \\ f \end{pmatrix},$$

where  $f, g_1, g_2$  are polynomials of degree greater than 2 in  $(X, Y, Z)$ , with

$$f(X, Y, Z) = -\frac{1}{4} (2\Gamma(Z) - 3) (2\sqrt{3}X + 2\sqrt{3}Y + 2\sqrt{3} - Z) Z^2 \quad (\text{B.1})$$

and with  $g_1, g_2$  not explicitly presented here due to their lengths. The center manifold is locally represented by

$$\{(X, Y) : X = h_1(Z), Y = h_2(Z), h_i(0) = 0, Dh_i(0) = 0, i = 1, 2\}, \quad (\text{B.2})$$

where  $h_1, h_2$  are approximated as

$$h_1(Z) = a_2 Z^2 + a_3 Z^3 + \mathcal{O}(Z^4), \quad (\text{B.3})$$

$$h_2(Z) = b_2 Z^2 + b_3 Z^3 + \mathcal{O}(Z^4), \quad (\text{B.4})$$

respectively. Due to the invariant property of the center manifold the vector function

$$\mathbf{h} = \begin{pmatrix} h_1 \\ h_2 \end{pmatrix}$$

has to satisfy a quasilinear partial differential equation given by

$$D\mathbf{h}(\mathbf{S}) [AS + \mathbf{F}(S, \mathbf{h}(S))] - B\mathbf{h}(S) - \mathbf{g}(S, \mathbf{h}(S)) = \mathbf{0}, \quad (\text{B.5})$$

with

$$\mathbf{g} = \begin{pmatrix} g_1 \\ g_2 \end{pmatrix}, \quad \mathbf{F} = f, \quad B = \begin{pmatrix} -3 & 0 \\ 0 & -3(w+1) \end{pmatrix}, \quad A = 0.$$

On substituting  $A$ ,  $\mathbf{h}$ ,  $\mathbf{F}$ ,  $B$ ,  $\mathbf{g}$  into equation (B.5) and equate the coefficients of all powers of  $Z$  to zero, we obtain the constants  $a_2$ ,  $a_3$ ,  $b_2$ ,  $b_3$  as

$$\begin{aligned} a_2 &= -\frac{\Gamma(0)}{6} + \frac{1}{3}, & a_3 &= -\frac{49\sqrt{3}}{144} + \frac{\sqrt{3}}{18}\Gamma(0) [7 - 2\Gamma(0)] - \frac{1}{6}\Gamma_z(0) \\ b_2 &= -\frac{1}{24}, & b_3 &= -\frac{\sqrt{3}}{144} [4\Gamma(0) - 7]. \end{aligned} \quad (\text{B.6})$$

The dynamics of the reduced system is ultimately determined by the equation

$$Z' = AZ + \mathbf{F}(Z, \mathbf{h}(Z)), \quad (\text{B.7})$$

and hence

$$S' = \sqrt{3} \left[ -\Gamma(0) + \frac{3}{2} \right] Z^2 + \left\{ \frac{1}{2} \left[ \Gamma(0) - \frac{3}{2} \right] - \sqrt{3}\Gamma_z(0) \right\} Z^3 + \mathcal{O}(Z^4). \quad (\text{B.8})$$

Therefore, for  $\Gamma(0) \neq \frac{3}{2}$ , point  $C_{3+}$  is saddle. However, if  $\Gamma(0) = \frac{3}{2}$  then the next terms in the expansion must be considered, in which case the point is stable if  $\Gamma_z(0) > 0$ .

A similar analysis for point  $A_{3-}(0, -1, 0)$  shows that it is saddle for  $\Gamma(0) \neq \frac{3}{2}$ , however for  $\Gamma(0) = \frac{3}{2}$  this point is stable if  $\Gamma_z(0) < 0$ .

The stability results of points  $A_{3\pm}$  are summarized in Table 2.

## References

- [1] SUPERNOVA SEARCH TEAM collaboration, A. G. Riess et al., *Observational evidence from supernovae for an accelerating universe and a cosmological constant*, *Astron. J.* **116** (1998) 1009–1038, [[astro-ph/9805201](#)].
- [2] SUPERNOVA COSMOLOGY PROJECT collaboration, S. Perlmutter et al., *Measurements of Omega and Lambda from 42 high redshift supernovae*, *Astrophys. J.* **517** (1999) 565–586, [[astro-ph/9812133](#)].
- [3] DES collaboration, T. M. C. Abbott et al., *Dark Energy Survey Year 1 Results: Cosmological Constraints from Galaxy Clustering and Weak Lensing*, **1708.01530**.
- [4] PLANCK collaboration, P. A. R. Ade et al., *Planck 2015 results. XIII. Cosmological parameters*, *Astron. Astrophys.* **594** (2016) A13, [[1502.01589](#)].
- [5] G. Bertone, D. Hooper and J. Silk, *Particle dark matter: Evidence, candidates and constraints*, *Phys. Rept.* **405** (2005) 279–390, [[hep-ph/0404175](#)].

- [6] L. Roszkowski, E. M. Sessolo and S. Trojanowski, *WIMP dark matter candidates and searches - current issues and future prospects*, [[1707.06277](#)].
- [7] N. Arkani-Hamed, D. P. Finkbeiner, T. R. Slatyer and N. Weiner, *A Theory of Dark Matter*, *Phys. Rev.* **D79** (2009) 015014, [[0808.0713](#)].
- [8] F. Y. Cyr-Racine and K. Sigurdson, *Cosmology of atomic dark matter*, *Phys. Rev.* **D87** (2013) 103515, [[1209.5752](#)].
- [9] K. Petraki, L. Pearce and A. Kusenko, *Self-interacting asymmetric dark matter coupled to a light massive dark photon*, *JCAP* **1407** (2014) 039, [[1403.1077](#)].
- [10] R. Foot and S. Vagnozzi, *Dissipative hidden sector dark matter*, *Phys. Rev.* **D91** (2015) 023512, [[1409.7174](#)].
- [11] R. Foot and S. Vagnozzi, *Diurnal modulation signal from dissipative hidden sector dark matter*, *Phys. Lett.* **B748** (2015) 61, [[1412.0762](#)].
- [12] R. Foot and S. Vagnozzi, *Solving the small-scale structure puzzles with dissipative dark matter*, *JCAP* **1607** (2016) 013, [[1602.02467](#)].
- [13] S. Weinberg, *The Cosmological Constant Problem*, *Rev. Mod. Phys.* **61** (1989) 1
- [14] V. Sahni, *The Cosmological constant problem and quintessence*, *Class. Quant. Grav.* **91** (2002) 3435, [[astro-ph/0202076](#)].
- [15] E. J. Copeland, M. Sami and S. Tsujikawa, *Dynamics of dark energy*, *Int. J. Mod. Phys.* **D15** (2006) 1753–1936, [[hep-th/0603057](#)].
- [16] Y.-F. Cai, E. N. Saridakis, M. R. Setare and J.-Q. Xia, *Quintom Cosmology: Theoretical implications and observations*, *Phys. Rept.* **493** (2010) 1–60, [[0909.2776](#)].
- [17] S. Nojiri and S. D. Odintsov, *Introduction to modified gravity and gravitational alternative for dark energy*, *eConf* **C0602061** (2006) 06, [[hep-th/0601213](#)].
- [18] S. Nojiri and S. D. Odintsov, *Unified cosmic history in modified gravity: from  $F(R)$  theory to Lorentz non-invariant models*, *Phys. Rept.* **505** (2011) 59–144, [[1011.0544](#)].
- [19] S. Tsujikawa, *Modified gravity models of dark energy*, *Lect. Notes Phys.* **800** (2010) 99–145, [[1101.0191](#)].
- [20] S. Capozziello and M. De Laurentis, *Extended Theories of Gravity*, *Phys. Rept.* **509** (2011) 167–321, [[1108.6266](#)].
- [21] Y.-F. Cai, S. Capozziello, M. De Laurentis and E. N. Saridakis,  *$f(T)$  teleparallel gravity and cosmology*, *Rept. Prog. Phys.* **79** (2016) 106901, [[1511.07586](#)].
- [22] S. Nojiri, S. D. Odintsov and V. K. Oikonomou, *Modified Gravity Theories on a Nutshell: Inflation, Bounce and Late-time Evolution*, *Phys. Rept.* **692** (2017) 1–104, [[1705.11098](#)].
- [23] A. H. Chamseddine and V. Mukhanov, *Mimetic Dark Matter*, *JHEP* **11** (2013) 135, [[1308.5410](#)].
- [24] L. Sebastiani, S. Vagnozzi and R. Myrzakulov, *Mimetic gravity: a review of recent developments and applications to cosmology and astrophysics*, *Adv. High Energy Phys.* **2017** (2017) 3156915, [[1612.08661](#)].
- [25] A. O. Barvinsky, *Dark matter as a ghost free conformal extension of Einstein theory*, *JCAP* **1401** (2014) 014, [[1311.3111](#)].
- [26] M. Chaichian, J. Kluson, M. Oksanen and A. Tureanu, *Mimetic dark matter, ghost instability and a mimetic tensor-vector-scalar gravity*, *JHEP* **12** (2014) 102, [[1404.4008](#)].
- [27] A. H. Chamseddine, V. Mukhanov and A. Vikman, *Cosmology with Mimetic Matter*, *JCAP* **1406** (2014) 017, [[1403.3961](#)].

- [28] S. Nojiri and S. D. Odintsov, *Mimetic  $F(R)$  gravity: inflation, dark energy and bounce*, *Mod. Phys. Lett. A* **29** (2014) 1450211, [[1408.3561](#)].
- [29] G. Leon and E. N. Saridakis, *Dynamical behavior in mimetic  $F(R)$  gravity*, *JCAP* **1504** (2015) 031, [[1501.00488](#)].
- [30] D. Momeni, A. Altaibayeva and R. Myrzakulov, *New Modified Mimetic Gravity*, *Int. J. Geom. Meth. Mod. Phys.* **11** (2014) 1450091, [[1407.5662](#)].
- [31] D. Momeni, R. Myrzakulov and E. Gudekli, *Cosmological viable mimetic  $f(R)$  and  $f(R, T)$  theories via Noether symmetry*, *Int. J. Geom. Meth. Mod. Phys.* **12** (2015) 1550101, [[1502.00977](#)].
- [32] A. V. Astashenok, S. D. Odintsov and V. K. Oikonomou, *Modified Gauss-Bonnet gravity with the Lagrange multiplier constraint as mimetic theory*, *Class. Quant. Grav.* **32** (2015) 185007, [[1504.04861](#)].
- [33] R. Myrzakulov, L. Sebastiani and S. Vagnozzi, *Inflation in  $f(R, \phi)$ -theories and mimetic gravity scenario*, *Eur. Phys. J. C* **75** (2015) 444, [[1504.07984](#)].
- [34] R. Myrzakulov, L. Sebastiani, S. Vagnozzi and S. Zerbini, *Mimetic covariant renormalizable gravity*, *Fund. J. Mod. Phys.* **8** (2015) 119–124, [[1505.03115](#)].
- [35] G. Cognola, R. Myrzakulov, L. Sebastiani, S. Vagnozzi and S. Zerbini, *Covariant Horava-like and mimetic Horndeski gravity: cosmological solutions and perturbations*, *Class. Quant. Grav.* **33** (2016) 225014, [[1601.00102](#)].
- [36] F. Arroja, N. Bartolo, P. Karmakar and S. Matarrese, *The two faces of mimetic Horndeski gravity: disformal transformations and Lagrange multiplier*, *JCAP* **1509** (2015) 051, [[1506.08575](#)].
- [37] Z. Haghani, T. Harko, H. R. Sepangi and S. Shahidi, *The scalar Einstein-aether theory*, [1404.7689](#).
- [38] Y. Rabochaya and S. Zerbini, *A note on a mimetic scalar-tensor cosmological model*, *Eur. Phys. J. C* **76** (2016) 85, [[1509.03720](#)].
- [39] R. Myrzakulov and L. Sebastiani, *Non-local  $F(R)$ -mimetic gravity*, *Astrophys. Space Sci.* **361** (2016) 188, [[1601.04994](#)].
- [40] S. D. Odintsov and V. K. Oikonomou, *Unimodular Mimetic  $F(R)$  Inflation*, *Astrophys. Space Sci.* **361** (2016) 236, [[1602.05645](#)].
- [41] M. Bouhmadi-Lopez, C.-Y. Chen and P. Chen, *Primordial Cosmology in Mimetic Born-Infeld Gravity*, [1709.09192](#).
- [42] C.-Y. Chen, M. Bouhmadi-Lopez and P. Chen, *Black hole solutions in mimetic Born-Infeld gravity*, [1710.10638](#).
- [43] F. Capela and S. Ramazanov, *Modified Dust and the Small Scale Crisis in CDM*, *JCAP* **1504** (2015) 051, [[1412.2051](#)].
- [44] L. Mirzaghali and A. Vikman, *Imperfect Dark Matter*, *JCAP* **1506** (2015) 028, [[1412.7136](#)].
- [45] S. Ramazanov, *Initial Conditions for Imperfect Dark Matter*, *JCAP* **1512** (2015) 007, [[1507.00291](#)].
- [46] N. A. Koshelev, *Effective dark matter fluid with higher derivative corrections*, [1512.07097](#).
- [47] S. A. Paston, *Forms of action for perfect fluid in general relativity and mimetic gravity*, [1708.03944](#).
- [48] S. Hirano, S. Nishi and T. Kobayashi, *Healthy imperfect dark matter from effective theory of mimetic cosmological perturbations*, *JCAP* **1707** (2017) 009, [[1704.06031](#)].

- [49] Y. Zheng, L. Shen, Y. Mou and M. Li, *On (in)stabilities of perturbations in mimetic models with higher derivatives*, *JCAP* **1708** (2017) 040, [[1704.06834](#)].
- [50] Y. Cai and Y.-S. Piao, *Higher order derivative coupling to gravity and its cosmological implications*, [1707.01017](#).
- [51] K. Takahashi and T. Kobayashi, *Extended mimetic gravity: Hamiltonian analysis and gradient instabilities*, [1708.02951](#).
- [52] M. A. Gorji, S. A. Hosseini Mansoori and H. Firouzjahi, *Higher Derivative Mimetic Gravity*, [1709.09988](#).
- [53] E. N. Saridakis and M. Tsoukalas, *Bi-scalar modified gravity and cosmology with conformal invariance*, *JCAP* **1604** (2016) 017, [[1602.06890](#)].
- [54] R. Kimura, A. Naruko and D. Yoshida, *Extended vector-tensor theories*, *JCAP* **1701** (2017) 002, [[1608.07066](#)].
- [55] N. Sadeghnezhad and K. Nozari, *Braneworld Mimetic Cosmology*, *Phys. Lett.* **B769** (2017) 134–140, [[1703.06269](#)].
- [56] A. H. Chamseddine and V. Mukhanov, *Resolving Cosmological Singularities*, *JCAP* **1703** (2017) 009, [[1612.05860](#)].
- [57] A. H. Chamseddine and V. Mukhanov, *Nonsingular Black Hole*, *Eur. Phys. J.* **C77** (2017) 183, [[1612.05861](#)].
- [58] S. Vagnozzi, *Recovering a MOND-like acceleration law in mimetic gravity*, *Class. Quant. Grav.* **34** (2017) 185006, [[1708.00603](#)].
- [59] L. Shen, Y. Mou, Y. Zheng and M. Li, *Direct couplings of mimetic dark matter and their cosmological effects*, [1710.03945](#).
- [60] J. Matsumoto, S. D. Odintsov and S. V. Sushkov, *Cosmological perturbations in a mimetic matter model*, *Phys. Rev.* **D91** (2015) 064062, [[1501.02149](#)].
- [61] S. Ramazanov, F. Arroja, M. Celoria, S. Matarrese and L. Pilo, *Living with ghosts in Horava-Lifshitz gravity*, *JHEP* **06** (2016) 020, [[1601.05405](#)].
- [62] D. Yoshida, J. Quintin, M. Yamaguchi and R. H. Brandenberger, *Cosmological perturbations and stability of nonsingular cosmologies with limiting curvature*, *Phys. Rev.* **D96** (2017) 043502, [[1704.04184](#)].
- [63] F. Arroja, N. Bartolo, P. Karmakar and S. Matarrese, *Cosmological perturbations in mimetic Horndeski gravity*, *JCAP* **1604** (2016) 042, [[1512.09374](#)].
- [64] S. D. Odintsov and V. K. Oikonomou, *Dark Energy Oscillations in Mimetic  $F(R)$  Gravity*, *Phys. Rev.* **D94** (2016) 044012, [[1608.00165](#)].
- [65] H. Firouzjahi, M. A. Gorji and S. A. Hosseini Mansoori, *Instabilities in Mimetic Matter Perturbations*, *JCAP* **1707** (2017) 031, [[1703.02923](#)].
- [66] J. Ben Achour, D. Langlois and K. Noui, *Degenerate higher order scalar-tensor theories beyond Horndeski and disformal transformations*, *Phys. Rev.* **D93** (2016) 124005, [[1602.08398](#)].
- [67] O. Malaeb, *Hamiltonian Formulation of Mimetic Gravity*, *Phys. Rev.* **D91** (2015) 103526, [[1404.4195](#)].
- [68] Z. Haghani, S. Shahidi and M. Shiravand, *Energy conditions in mimetic- $f(R)$  gravity*, [1507.07726](#).
- [69] D. Langlois and K. Noui, *Hamiltonian analysis of higher derivative scalar-tensor theories*, *JCAP* **1607** (2016) 016, [[1512.06820](#)].
- [70] A. Ijjas, J. Ripley and P. J. Steinhardt, *NEC violation in mimetic cosmology revisited*, *Phys. Lett.* **B760** (2016) 132–138, [[1604.08586](#)].

- [71] J. Kluson, *Canonical Analysis of Inhomogeneous Dark Energy Model and Theory of Limiting Curvature*, *JHEP* **03** (2017) 031, [[1701.08523](#)].
- [72] H. Saadi, *A Cosmological Solution to Mimetic Dark Matter*, *Eur. Phys. J.* **C76** (2016) 14, [[1411.4531](#)].
- [73] Z. Haghani, T. Harko, H. R. Sepangi and S. Shahidi, *Cosmology of a Lorentz violating Galileon theory*, *JCAP* **1505** (2015) 022, [[1501.00819](#)].
- [74] K. Hammer and A. Vikman, *Many Faces of Mimetic Gravity*, [1512.09118](#).
- [75] S. Nojiri, S. Odintsov and V. Oikonomou, *Viable Mimetic Completion of Unified Inflation-Dark Energy Evolution in Modified Gravity*, *Phys. Rev.* **D94** (2016) 104050, [[1608.07806](#)].
- [76] E. H. Baffou, M. J. S. Houndjo, M. Hamani-Daouda and F. G. Alvarenga, *Late time cosmological approach in mimetic  $f(R, T)$  gravity*, [1706.08842](#).
- [77] M. Raza, K. Myrzakulov, D. Momeni and R. Myrzakulov, *Mimetic Attractors*, *Int. J. Theor. Phys.* **55** (2016) 2558, [[1508.00971](#)].
- [78] N. Deruelle and J. Rua, *Disformal Transformations, Veiled general relativity and Mimetic Gravity*, *JCAP* **1409** (2014) 002, [[1407.0825](#)].
- [79] R. Myrzakulov and L. Sebastiani, *Spherically symmetric static vacuum solutions in Mimetic gravity*, *Gen. Rel. Grav.* **47** (2015) 89, [[1503.04293](#)].
- [80] A. Addazi and A. Marciano, *Evaporation and Antieaporation instabilities*, [1710.07962](#).
- [81] D. Momeni, P. H. R. S. Moraes, H. Gholizade and R. Myrzakulov, *Mimetic Compact Stars*, [1505.05113](#).
- [82] A. V. Astashenok and S. D. Odintsov, *From neutron stars to quark stars in mimetic gravity*, *Phys. Rev.* **D94** (2016) 063008, [[1512.07279](#)].
- [83] R. Myrzakulov, L. Sebastiani, S. Vagnozzi and S. Zerbini, *Static spherically symmetric solutions in mimetic gravity: rotation curves and wormholes*, *Class. Quant. Grav.* **33** (2016) 125005, [[1510.02284](#)].
- [84] E. Babichev and S. Ramazanov, *Gravitational focusing of Imperfect Dark Matter*, *Phys. Rev.* **D95** (2017) 024025, [[1609.08580](#)].
- [85] F. Arroja, T. Okumura, N. Bartolo, P. Karmakar and S. Matarrese, *Large-scale structure in mimetic Horndeski gravity*, [1708.01850](#).
- [86] J. M. Ezquiaga and M. Zumalacarregui, *Dark Energy After GW170817: Dead Ends and the Road Ahead*, *Phys. Rev. Lett.* **119** no. 25 (2017) 251304, [[1710.05901](#)].
- [87] P. Creminelli and F. Vernizzi, *Dark Energy after GW170817 and GRB170817A*, *Phys. Rev. Lett.* **119** no. 25 (2017) 251302, [[1710.05877](#)].
- [88] J. Sakstein and B. Jain, *Implications of the Neutron Star Merger GW170817 for Cosmological Scalar-Tensor Theories*, *Phys. Rev. Lett.* **119** no. 25 (2017) 251303, [[1710.05893](#)].
- [89] T. Baker, E. Bellini, P. G. Ferreira, M. Lagos, J. Noller and I. Sawicki, *Strong constraints on cosmological gravity from GW170817 and GRB 170817A*, *Phys. Rev. Lett.* **119** no. 25 (2017) 251301, [[1710.06394](#)].
- [90] D. Langlois, R. Saito, D. Yamauchi and K. Noui, *Scalar-tensor theories and modified gravity in the wake of GW170817*, [1711.07403](#).
- [91] L. Visinelli, N. Bolis and S. Vagnozzi, *Probing extra dimensions with gravitational and electromagnetic signals from compact mergers*, [1711.06628](#).
- [92] M. Rinaldi, L. Sebastiani, A. Casalino and S. Vagnozzi, *Mimicking dark matter and dark energy in a mimetic model compatible with GW170817*, in preparation (2018).

- [93] A. Casalino, M. Rinaldi, L. Sebastiani and S. Vagnozzi, *Mimetic gravity in light of GW170817*, in preparation (2018).
- [94] T. Jacobson and A. J. Speranza, *Variations on an aethereal theme*, *Phys. Rev.* **D92** (2015) 044030, [[1503.08911](#)].
- [95] A. H. Chamseddine, A. Connes and V. Mukhanov, *Quanta of Geometry: Noncommutative Aspects*, *Phys. Rev. Lett.* **114** (2015) 091302, [[1409.2471](#)].
- [96] S. Chinaglia, A. Collaux and S. Zerbini, *A non-polynomial gravity formulation for Loop Quantum Cosmology bounce*, [1708.08667](#).
- [97] E. Guendelman, E. Nissimov and S. Pacheva, *Unified Dark Energy and Dust Dark Matter Dual to Quadratic Purely Kinetic K-Essence*, *Eur. Phys. J.* **C76** (2016) 90, [[1511.07071](#)].
- [98] D. Benisty and E. I. Guendelman, *Interacting Diffusive Unified Dark Energy and Dark Matter from Scalar Fields*, *Eur. Phys. J.* **C77** (2017) 396, [[1701.08667](#)].
- [99] M. Kopp, C. Skordis and D. B. Thomas, *Extensive investigation of the generalized dark matter model*, *Phys. Rev.* **D94** (2016) 043512, [[1605.00649](#)].
- [100] M. Ali, V. Husain, S. Rahmati and J. Ziprick, *Linearized gravity with matter time*, *Class. Quant. Grav.* **33** (2016) 105012, [[1512.07854](#)].
- [101] D. Benisty and E. I. Guendelman, *A transition between bouncing hyper-inflation to  $\Lambda$ CDM from diffusive scalar fields*, [1710.10588](#).
- [102] A. A. Coley, *Dynamical systems and cosmology*, vol. 291. Kluwer, Dordrecht, Netherlands, 2003, [10.1007/978-94-017-0327-7](#).
- [103] G. Leon and C. R. Fadrakas, *Cosmological dynamical systems*. LAP Lambert Academic Publishing, 2012.
- [104] C. G. Boehmer and N. Chan, *Dynamical systems in cosmology*, 2014, [[1409.5585](#)].
- [105] S. Bahamonde, C. G. Boehmer, S. Carloni, E. J. Copeland, W. Fang and N. Tamanini, 2017 [[1712.03107](#)].
- [106] E. J. Copeland, A. R. Liddle and D. Wands, *Exponential potentials and cosmological scaling solutions*, *Phys. Rev.* **D57** (1998) 4686–4690, [[gr-qc/9711068](#)].
- [107] S. Carloni, P. K. S. Dunsby, S. Capozziello and A. Troisi, *Cosmological dynamics of  $R^{**n}$  gravity*, *Class. Quant. Grav.* **22** (2005) 4839, [[gr-qc/0410046](#)].
- [108] S. Carloni, S. Capozziello, J. A. Leach and P. K. S. Dunsby, *Cosmological dynamics of scalar-tensor gravity*, *Class. Quant. Grav.* **25** (2008) 035008, [[gr-qc/0701009](#)].
- [109] G. Leon and E. N. Saridakis, *Phase-space analysis of Horava-Lifshitz cosmology*, *JCAP* **0911** (2009) 006, [[0909.3571](#)].
- [110] C. Xu, E. N. Saridakis and G. Leon, *Phase-Space analysis of Teleparallel Dark Energy*, *JCAP* **1207** (2012) 005, [[1202.3781](#)].
- [111] G. Leon and E. N. Saridakis, *Dynamical analysis of generalized Galileon cosmology*, *JCAP* **1303** (2013) 025, [[1211.3088](#)].
- [112] G. Leon, J. Saavedra and E. N. Saridakis, *Cosmological behavior in extended nonlinear massive gravity*, *Class. Quant. Grav.* **30** (2013) 135001, [[1301.7419](#)].
- [113] G. Kofinas, G. Leon and E. N. Saridakis, *Dynamical behavior in  $f(T, T_G)$  cosmology*, *Class. Quant. Grav.* **31** (2014) 175011, [[1404.7100](#)].
- [114] C. G. Boehmer, N. Tamanini and M. Wright, *Interacting quintessence from a variational approach Part I: algebraic couplings*, *Phys. Rev.* **D91** (2015) 123002, [[1501.06540](#)].

- [115] C. G. Boehmer, N. Tamanini and M. Wright, *Interacting quintessence from a variational approach Part II: derivative couplings*, *Phys. Rev.* **D91** (2015) 123003, [[1502.04030](#)].
- [116] S. Carloni, T. Koivisto and F. S. N. Lobo, *Dynamical system analysis of hybrid metric-Palatini cosmologies*, *Phys. Rev.* **D92** (2015) 064035, [[1507.04306](#)].
- [117] J. Dutta, W. Khyllep and N. Tamanini, *Cosmological dynamics of scalar fields with kinetic corrections: Beyond the exponential potential*, *Phys. Rev.* **D93** (2016) 063004, [[1602.06113](#)].
- [118] S. Carloni, F. S. N. Lobo, G. Otalora and E. N. Saridakis, *Dynamical system analysis for a nonminimal torsion-matter coupled gravity*, *Phys. Rev.* **D93** (2016) 024034, [[1512.06996](#)].
- [119] N. Tamanini and M. Wright, *Cosmological dynamics of extended chameleons*, *JCAP* **1604** (2016) 032, [[1602.06903](#)].
- [120] J. Dutta, W. Khyllep and N. Tamanini, *Scalar-Fluid interacting dark energy: cosmological dynamics beyond the exponential potential*, *Phys. Rev.* **D95** (2017) 023515, [[1701.00744](#)].
- [121] S. Carloni and J. P. Mimoso, *Phase space of modified Gauss-Bonnet gravity*, *Eur. Phys. J.* **C77** (2017) 547, [[1701.00231](#)].
- [122] J. Dutta, W. Khyllep and N. Tamanini, *Dark energy with a gradient coupling to the dark matter fluid: cosmological dynamics and structure formation*, [[1707.09246](#)].
- [123] H. Zonunmawia, W. Khyllep, N. Roy, J. Dutta and N. Tamanini, *Extended Phase Space Analysis of Interacting Dark Energy Models in Loop Quantum Cosmology*, *Phys. Rev.* **D96** (2017) 083527, [[1708.07716](#)].
- [124] M. Hohmann, L. Jarv and U. Ualikhanova, *Dynamical systems approach and generic properties of  $f(T)$  cosmology*, *Phys. Rev.* **D96** (2017) 043508, [[1706.02376](#)].
- [125] E. A. Lim, I. Sawicki and A. Vikman, *Dust of Dark Energy*, *JCAP* **1005** (2010) 012, [[1003.5751](#)].
- [126] C. Gao, Y. Gong, X. Wang and X. Chen, *Cosmological models with Lagrange Multiplier Field*, *Phys. Lett.* **B702** (2011) 107–113, [[1003.6056](#)].
- [127] S. Capozziello, J. Matsumoto, S. Nojiri and S. D. Odintsov, *Dark energy from modified gravity with Lagrange multipliers*, *Phys. Lett.* **B693** (2010) 198–208, [[1004.3691](#)].
- [128] A. Golovnev, *On the recently proposed Mimetic Dark Matter*, *Phys. Lett.* **B728** (2014) 39–40, [[1310.2790](#)].
- [129] J. D. Bekenstein, *The Relation between physical and gravitational geometry*, *Phys. Rev.* **D48** (1993) 3641–3647, [[gr-qc/9211017](#)].
- [130] F.-F. Yuan and P. Huang, *Induced geometry from disformal transformation*, *Phys. Lett.* **B744** (2015) 120–124, [[1501.06135](#)].
- [131] G. Domenech, A. Naruko and M. Sasaki, *Cosmological disformal invariance*, *JCAP* **1510** (2015) 067, [[1505.00174](#)].
- [132] C. Deffayet, G. Esposito-Farese and D. A. Steer, *Counting the degrees of freedom of generalized Galileons*, *Phys. Rev.* **D92** (2015) 084013, [[1506.01974](#)].
- [133] G. Domenech, S. Mukohyama, R. Namba, A. Naruko, R. Saitou and Y. Watanabe, *Derivative-dependent metric transformation and physical degrees of freedom*, *Phys. Rev.* **D92** (2015) 084027, [[1507.05390](#)].
- [134] R. Saitou, *Canonical invariance of spatially covariant scalar-tensor theory*, *Phys. Rev.* **D94** (2016) 104054, [[1604.03847](#)].
- [135] M. Celoria, S. Matarrese and L. Pilo, *Disformal invariance of continuous media with linear equation of state*, *JCAP* **1702** (2017) 004, [[1609.08507](#)].

- [136] J. M. Ezquiaga, J. Garcia-Bellido and M. Zumalacarregui, *Field redefinitions in theories beyond Einstein gravity using the language of differential forms*, *Phys. Rev.* **D95** (2017) 084039, [[1701.05476](#)].
- [137] K. Takahashi, H. Motohashi, T. Suyama and T. Kobayashi, *general invertible transformation and physical degrees of freedom*, *Phys. Rev.* **D95** (2017) 084053, [[1702.01849](#)].
- [138] M. Crisostomi, K. Noui, C. Charmousis and D. Langlois, *Beyond Lovelock: on higher derivative metric theories*, [1710.04531](#).
- [139] Y. L. Bolotin, A. Kostenko, O. A. Lemets and D. A. Yerokhin, *Cosmological Evolution With Interaction Between Dark Energy And Dark Matter*, *Int. J. Mod. Phys.* **D24** no. 03 (2014) 1530007, [[1310.0085](#)].
- [140] L. Amendola, *Coupled quintessence*, *Phys. Rev.* **D62** (2000) 043511, [[astro-ph/9908023](#)].
- [141] B. Wang, E. Abdalla, F. Atrio-Barandela and D. Pavon, *Dark Matter and Dark Energy Interactions: Theoretical Challenges, Cosmological Implications and Observational Signatures*, *Rept. Prog. Phys.* **79** no. 9 (2017) 096901, [[1603.08299](#)].
- [142] R. C. Nunes, S. Pan and E. N. Saridakis, *New constraints on interacting dark energy from cosmic chronometers*, *Phys. Rev.* **D94** (2016) 023508, [[1605.01712](#)].
- [143] VIRGO, LIGO SCIENTIFIC collaboration, B. P. Abbott et al., *GW170817: Observation of Gravitational Waves from a Binary Neutron Star Inspiral*, *Phys. Rev. Lett.* **119** (2017) 161101, [[1710.05832](#)].
- [144] N. Tamanini, *Dynamics of cosmological scalar fields*, *Phys. Rev.* **D89** (2014) 083521, [[1401.6339](#)].
- [145] M. Quartin, M. O. Calvao, S. E. Joras, R. R. R. Reis and I. Waga, *Dark Interactions and Cosmological Fine-Tuning*, *JCAP* **0805** (2008) 007, [[0802.0546](#)].
- [146] N. Tamanini, *Phenomenological models of dark energy interacting with dark matter*, *Phys. Rev.* **D92** (2015) 043524, [[1504.07397](#)].
- [147] S. Vagnozzi, E. Giusarma, O. Mena, K. Freese, M. Gerbino, S. Ho and M. Lattanzi, *Unveiling  $\nu$  secrets with cosmological data: neutrino masses and mass hierarchy*, *Phys. Rev.* **D96** (2017) 123503, [[1701.08172](#)].
- [148] S. Vagnozzi, S. Dhawan, M. Gerbino, K. Freese, A. Goobar and O. Mena, *Constraints on the sum of the neutrino masses in dynamical dark energy models with  $w(z) \geq -1$  are tighter than those obtained in  $\Lambda$ CDM*, [1801.08553](#).